Volume 6 SEPTEMBER, 1935 Number 9

PHYSICS

A Journal of General and Applied Physics

Heat Treatment of Magnetic Materials in a Magnetic Field

I. Survey of Iron-Cobalt-Nickel Alloys

JOY F. DILLINGER AND RICHARD M. BOZORTH, *Bell Telephone Laboratories*

(Received June 10, 1935)

The changes that occur in the magnetic properties of iron-cobalt-nickel alloys when they are annealed in a magnetic field, have been investigated for a series of these alloys. The maximum change for the iron-nickel alloys occurs between 65 and 70 percent nickel and is evidenced by a large increase in maximum permeability and a hysteresis loop of rectangular shape. All of the alloys with Curie points above 500°C and with no phase transformation have their properties similarly changed. Thorough preliminary annealing enhances the effect. With an extreme preliminary anneal of 1400°C for 18 hours specimens of 65 permalloy have been obtained with the record value of maximum permeability of 600,000. The magnetic characteristics of materials treated in this way are relatively insensitive to stress. These magnetic characteristics are, however, highly anisotropic; the maximum permeability in one direction is as much as 150 times as large as that at right angles.

INTRODUCTION

IT has been known for many years[1] that the magnetic properties of iron and silicon steel are somewhat changed by heat treating in a magnetic field. During the early experiments with perminvar[2] it was found[3] that the constant permeability for which this material is best known could be obtained only when there was no field present during the heat treatment, and that when a field of one oersted was maintained during annealing the maximum permeability at room temperature was 136,000 instead of the usual value of 1500. More recently, during experiments on the Barkhausen effect in straight fine wires (0.03 mm in diameter) it was found that the hysteresis loops for these specimens had square corners and vertical sides. Investigation showed that these properties were caused by the presence of a magnetic field in the furnace in which they were heat treated. At that time the experiments of Kelsall[4] were known to us and it was decided to make a more thorough study of the effect of heat treating alloys in a magnetic field.

Accordingly we have performed the experiments described below, mainly on iron-cobalt-nickel alloys, and have made a rather detailed study[5] of two of them. We have found that the magnetic properties of many of these alloys are greatly changed by heat treatment in a magnetic field. In some specimens the maximum permeability is increased from 5000 to 300,000, in others from 20,000 to 600,000.

PROCEDURE

The samples tested were rings, 8 cm in diameter, 0.015 cm in radial thickness and 0.32 cm wide, made from one turn of tape overlapped about 0.4 cm and spotwelded. The tape was fabricated as described by Elmen.[2] These samples were annealed in hydrogen in a metal pot. Commercial hydrogen, filtered through hot palladium-asbestos to remove the free oxygen, was passed slowly through the pot during the anneal.

[1] H. Pender and R. L. Jones, Phys. Rev. **1**, 259 (1913).
[2] G. W. Elmen, J. Frank. Inst. **206**, 317 (1928).
[3] P. P. Cioffi, U. S. Patent 1708936 (1929).
[4] G. A. Kelsall, Physics **5**, 169 (1934).

[5] See the succeeding paper, this issue.

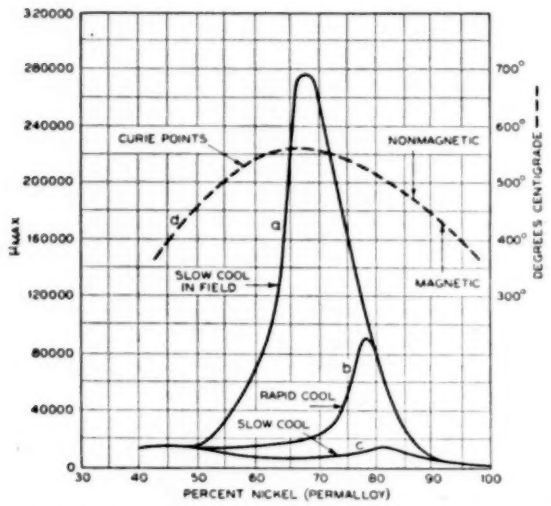

FIG. 1. The maximum permeabilites of iron-nickel alloys cooled in different ways after annealing at 1000°C. Curie points of the same alloys are shown by the dashed line.

The samples were first annealed at 1000°C for one hour and cooled in the furnace at a maximum rate of about 300°C/hour. Each sample was then placed in a torroidal lavite box and wound with deoxidized copper wire for magnetizing. This assembly was then given a second anneal in hydrogen at a maximum temperature of about 50°C above the Curie point of the specimen. This temperature was maintained for one hour and then the sample cooled in the furnace as before. While the sample was cooling from this second anneal a magnetizing field of 16 oersteds was applied.

After annealing each sample was placed in a torroidal box and two windings applied for magnetic measurements. These were made with a Haworth fluxmeter[6] and hysteresis loops were photographically recorded with the same instrument.

TABLE I. *Magnetic characteristics of iron-cobalt-nickel alloys.*

COMPOSITION	ANNEALED WITHOUT A FIELD		ANNEALED WITH A FIELD	
Fe-Co-Ni	H_c	μ_{max}	H_c	μ_{max}
10–20–70	1.16	1,490	0.28	11,600
10–39–51	2.54	2,440	0.69	7,100
11–59–30	3.86	1,110	2.28	5,300
11–78–11	3.56	1,730	2.54	4,100
30–25–45	0.90	2,000	0.09	115,000
30–44–26	2.90	1,150	0.74	12,500
45–10–45	0.69	7,550	0.44	18,300
48–52	0.70	11,000	0.55	22,400

[6] F. E. Haworth, Bell Sys. Tech. J. **10**, 20 (1931).

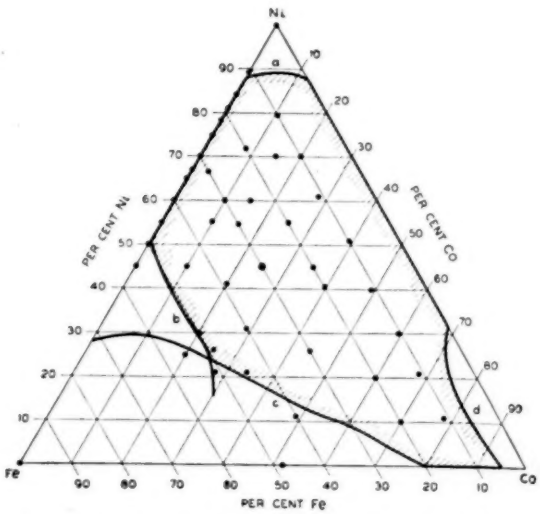

FIG. 2. The alloys investigated. The magnetic properties of the compositions within the shaded area are changed by annealing in a magnetic field. Curves (a) and (b) represent compositions with Curie points of 500°C. Curves (c) and (d) represent compositions with phase transformations near room temperature.

MAGNETIC CHARACTERISTICS

In Fig. 1, curve (a) gives the maximum permeabilities of a series of iron-nickel alloys cooled in a magnetic field as described above. Curves (b) and (c) give for comparison permeabilities obtained[7] when similar alloys are slowly cooled or rapidly cooled without an applied field. The dotted curve (d) gives the Curie points of the iron-nickel alloys here used. It is apparent that curves (a) and (d) have maxima between 65 and 70 percent nickel, and that μ_{max} for alloys with low Curie points is not noticeably changed by cooling in a magnetic field.

We have also found that the magnetic characteristics of many of the iron-cobalt-nickel alloys are changed when they are cooled in a magnetic field. All of the alloys tested which have compositions lying within the outlined area shown in Fig. 2 are affected by such treatment. Some compositions outside of this area near the iron-cobalt line are still under investigation. Of these iron, and the alloy with 48 percent Fe and 52 percent Co, show some changes. The points on the diagram indicate the alloys tested.

Here again it was found that alloys with high Curie points are affected by cooling in a magnetic

[7] G. W. Elmen, J. Frank. Inst. **207**, 583 (1929), and more recent data by G. A. Kelsall.

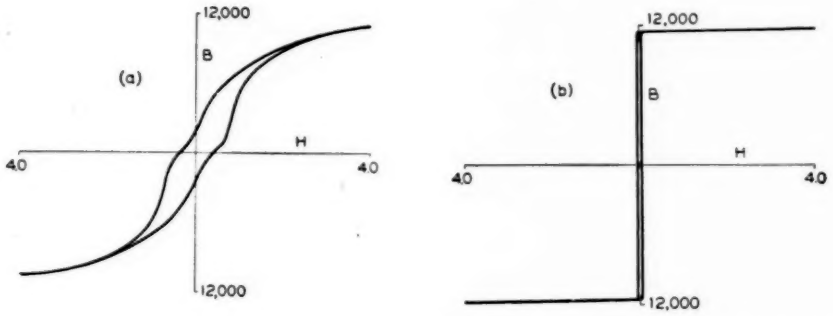

FIG. 3. Hysteresis loops of 65 permalloy cooled in different ways from 1000°C. For loop (a) no field was applied during cooling; for loop (b) a field of 10 oersteds was maintained during cooling.

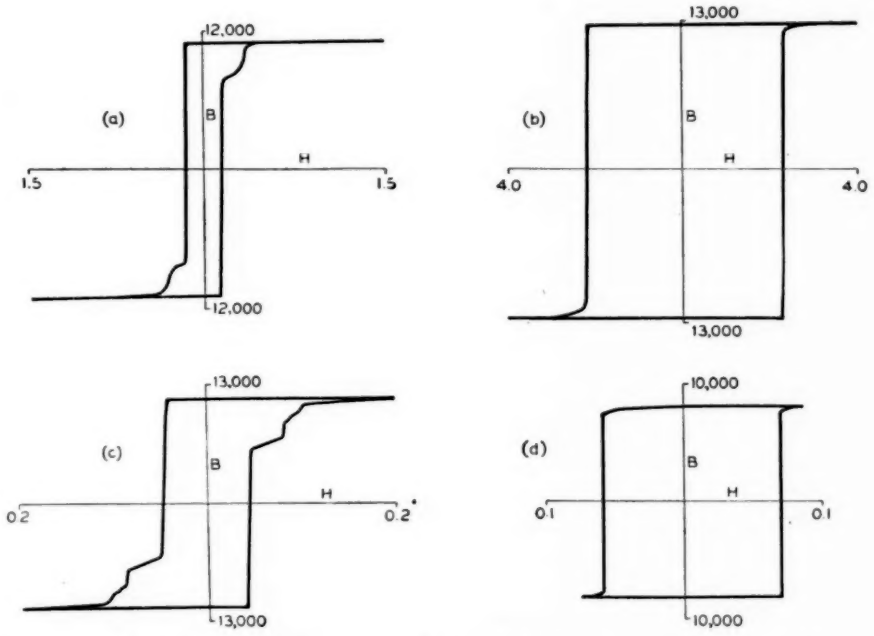

FIG. 4. Hysteresis loops of different materials annealed in a magnetic field: (a) 25 percent Fe, 15 percent Co, 60 percent Ni; (b) 20 percent Fe, 70 percent Co, 10 percent Ni; (c) 65 permalloy fine wire; (d) 15 percent Fe, 15 percent Co, 70 percent Ni.

field. Curves (a) and (b) in Fig. 2 indicate alloys with Curie points of 500°C. Curves (c) and (d) indicate alloys with phase transformations near room temperature.

Table I gives the values of coercivity, H_c, and maximum permeability, μ_{max}, of representative alloys. The values for the identical tape annealed without an applied field were kindly furnished by G. A. Kelsall. The conventional magnetic characteristics given in Table I do not, however, give a complete picture of the peculiar cyclic magnetic properties of these alloys, which are shown by their hysteresis loops.

HYSTERESIS LOOPS

The shape of the hysteresis loop is often very radically changed by treatment in a field. The two loops in Fig. 3 show this for specimens of 65 percent Ni, 35 percent Fe (65 permalloy). Loop (a) was taken for a specimen annealed without the application of a field and loop (b) for one annealed in a field. The square corners and

vertical sides that are present in exaggerated form in the latter condition are characteristic of the loops of materials affected by this treatment. The vertical sides represent changes in magnetic flux which are not instantaneous. The time necessary for these flux changes depends upon the dimensions of the sample and upon the excess of the applied field over the coercivity. In Fig. 3(b) the time required for the flux to change along each of the vertical sides was about one minute when the applied field was held constant at H_c.

Other alloys annealed in a field give hysteresis loops that are very different from those usually found. Some loops of this type are shown in Fig. 4. Loop (a) is for a specimen containing 25 percent Fe, 15 percent Co and 60 percent Ni. An alloy containing 20 percent Fe, 70 percent Co, 10 percent Ni was used for loop (b). Loop (c) is for a 0.051 cm wire of 65 permalloy, and loop (d) is for a specimen containing 15 percent Fe, 15 percent Co and 70 percent Ni.

It is impossible to demagnetize completely many of the samples that have loops with vertical sides. The sample of Fig. 3(b) could be demagnetized only partially and others could not be demagnetized much below their remanence even by reducing the reversed field in steps as small as 0.003 oersted, or by an alternating field continuously decreasing in amplitude.

The maximum value of intensity of magnetization obtainable for alloys annealed in a field is no larger than for similar alloys annealed without the application of a field. Approximate saturation is obtained, however, for the former with very much lower applied fields than for the latter.

Stress Sensitivity

It is well known that the application of stress to many of these alloys will produce hysteresis loops that are nearly rectangular.[8] In the case of 65 permalloy in tension a loop very similar in shape to that given in Fig. 3(b) is obtained. From this it was thought that the hysteresis loop of this alloy annealed in a field would not change with the application of tension. To test this, two straight samples of 65 permalloy tape 60 cm long were annealed. One was annealed in a field of 10 oersteds and the other was annealed in zero field (the earth's field was compensated). Measurements were made in a magnetic yoke[9] in such a way that tension could be applied during measurement. The maximum permeabilities as a function of the stress applied are given in Fig. 5. Here it is seen that, as predicted, the specimen annealed in a field was affected relatively little by tension.

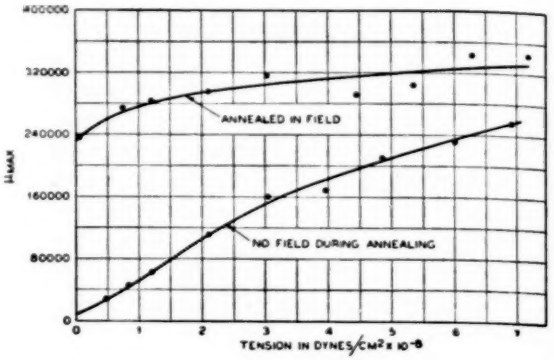

FIG. 5. The effect of tension upon the maximum permeabilities of samples of 65 permalloy annealed with and without an applied magnetic field.

In straight pieces of thin tape and of fine wire annealed in a field the sudden magnetic changes (corresponding to the vertical sides of loops) were found to travel along the sample at a definite velocity in a manner very similar to that observed by Sixtus and Tonks[10] and others in strained wires.

Temperature of Anneal

The temperature at which the material is annealed has much to do with the maximum permeability and the shape of the hysteresis loop. This is well illustrated by the following results. Similar ring samples of hard rolled 65 permalloy tape were annealed for one hour at given temperatures and then cooled to room temperature in an applied magnetic field. The values of maximum permeability obtained in this way are plotted in Fig. 6(a) against the

[8] F. Preisach, Ann. d. Physik **3**, 737 (1929). See also references 9 and 10, as well as the earlier paper by R. Forrer, Comptes rendus **180**, 1394 (1925).

[9] O. E. Buckley and L. W. McKeehan, Phys. Rev. **26**, 261 (1925).

[10] K. J. Sixtus and L. Tonks, Phys. Rev. **39**, 357 (1932), and earlier papers.

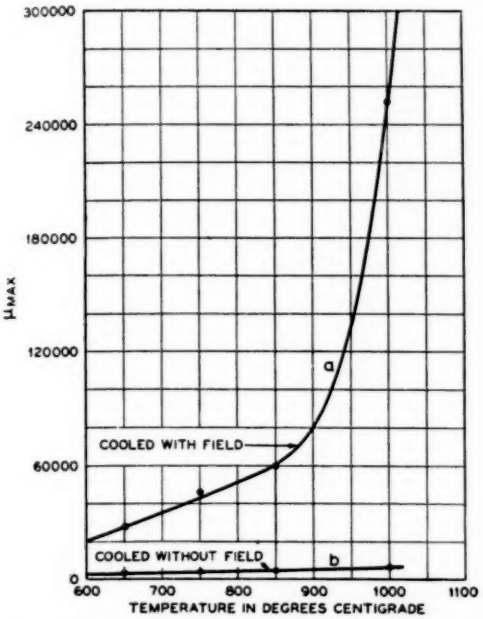

FIG. 6. The maximum permeabilities of samples of 65 permalloy, originally hard worked, after annealing at various temperatures for one hour and cooling with or without an applied field.

maximum temperature of the anneal. Curve (b) gives the maximum permeabilities on similar samples annealed without the application of a field. These results and others indicate that thorough annealing is necessary for maximum effects.

Temperatures higher than those given in Fig. 6 have been used in some experiments. In this case solid rings of 65 permalloy 2.86 cm O.D., 2.38 cm I.D. and 0.63 cm high were treated in hydrogen[11] at 1400°C for 18 hours and later reheated to 650°C and cooled in a magnetic field. Hysteresis loops and μ, H curves for one of these samples are given in Figs. 7 and 8. Curves (a) were taken after the high temperature treatment but before the treatment in a magnetic field. Curves (b) were taken after both treatments. The value of maximum permeability for this sample is the highest of which we have any record and the coercivity (0.012 oersted) is the lowest. The area of the loop indicates an energy loss of 50 ergs/cm³/cycle which is also a record low value for hysteresis losses. The time required for the flux to change along each of the vertical sides of this loop was about three minutes.

[11] By P. P. Cioffi, as described in Phys. Rev. **39**, 363 (1932).

ANISOTROPY

The magnetic properties of these materials are not the same in all directions. In the work described above, the magnetic field that was applied during measurement was parallel to the field applied during heat treatment. The effect of applying these two fields in mutually perpendicular directions was investigated for a seamless tube of perminvar (30 percent iron, 25 percent cobalt, 45 percent nickel) 60 cm long, 0.48 cm outside diameter, and 0.025 cm thick. This tube was annealed at 1000°C in hydrogen, and again at 650°C in a magnetic field applied parallel to the axis of the tube. Measurements were made with applied fields perpendicular to the axis by using a search coil wound through the ends of the tube and back along the outside and a magnetizing current passed through an insulated conductor along the axis of the tube. The values of permeability measured in this way are given in Fig. 9. The maximum permeability under these conditions is about 1250 and the hysteresis loop is

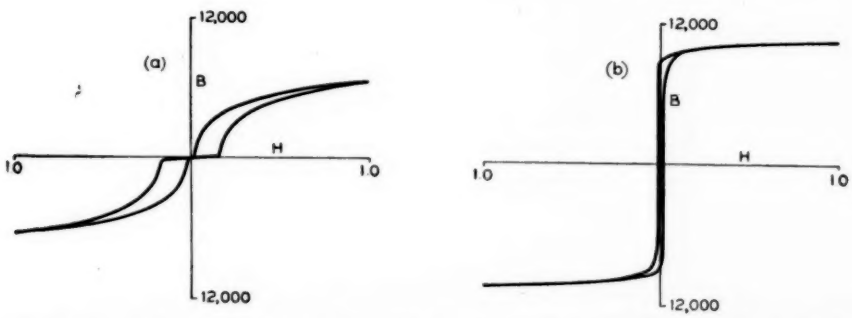

FIG. 7. Hysteresis loops of 65 permalloy: (a) After anneal at 1400°C for 18 hr. in hydrogen; (b) After further heating to 650°C and cooling in a magnetic field.

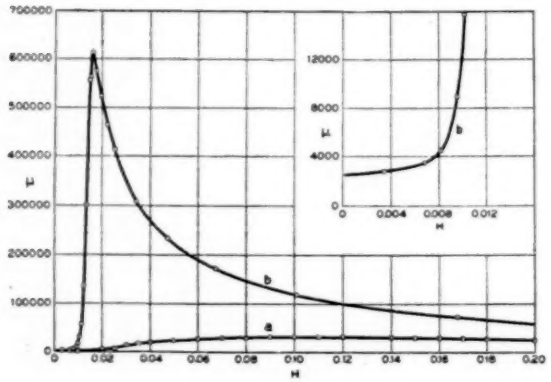

FIG. 8. Permeability curves for 65 permalloy, corresponding to the loops of Fig. 7.

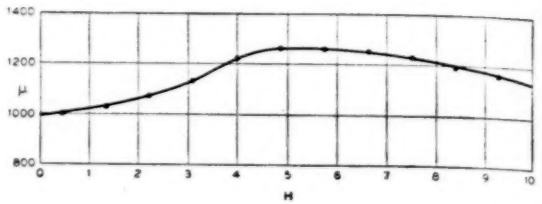

FIG. 9. Permeability curve for a tube of perminvar (30 percent Fe, 25 percent Co, 45 percent Ni) after cooling in a magnetic field applied at right angles to the field used for measurement.

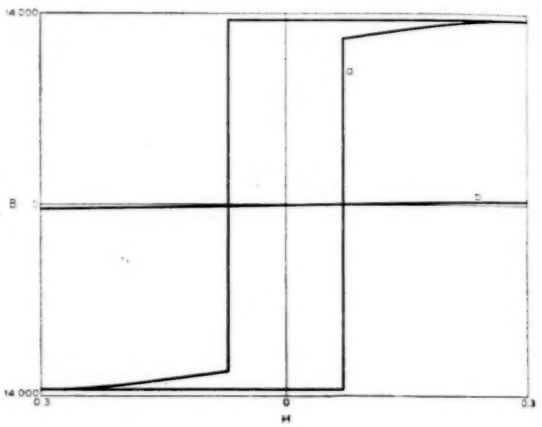

FIG. 10. Hysteresis loops of a tube of perminvar after cooling in a magnetic field: (a) Loop measured with field parallel to the field applied during heat treatment; (b) Loop measured with field perpendicular to the field applied during heat treatment.

nearly a straight line. If, however, the measuring field and the field applied during the anneal are parallel (circular) the maximum permeability on this sample is about 190,000 and the hysteresis loop is nearly a rectangle. The loops for these two situations are shown on the same scale in Fig. 10.

SUMMARY

Heat treatment of the binary iron-nickel alloys in a magnetic field is effective in a broad region near 65 percent nickel. Many of the iron-cobalt-nickel alloys are affected by this treatment. Specimens so treated are relatively insensitive to strains. Record values of maximum permeability, hysteresis loss and coercivity for a ferromagnetic material were obtained by applying this method to 65 permalloy with the field applied for measurement parallel to the field applied during heat treatment. The magnetic properties so obtained are conspicuously anisotropic.

In general, we have found that if this method of annealing in a magnetic field is to be effective the material must have a Curie point somewhat above 500°C, and must not have a phase change between about 500°C and room temperature. In any material, thorough preliminary annealing is essential for the best results.

We are inclined to the conclusion that the forces arising from magnetostriction produce plastic deformation if the Curie point is sufficiently high and that this results in magnetic orientation with high permeability in one direction and low permeability in directions at right angles. A complicated type of magnetostriction such as that existing in iron apparently reduces the efficacy of this type of treatment, since relatively small changes have been obtained in this material. The smallness of the changes produced in iron may also be affected by its small magnetostriction and by its greater resistance to plastic flow.

A more detailed discussion of these and other results is given in the following paper.

Heat Treatment of Magnetic Materials in a Magnetic Field

II. Experiments with Two Alloys

RICHARD M. BOZORTH AND JOY F. DILLINGER, *Bell Telephone Laboratories*

(Received June 10, 1935)

The magnetization of two alloys, as affected by heat treatment in a magnetic field at various temperatures, is examined in some detail in order to elucidate the nature of the accompanying changes which result in some cases in a 30-fold increase in maximum permeability. The *experiments* show that these alloys (one containing approximately 35 percent iron and 65 percent nickel, the other 20 percent iron, 60 percent cobalt and 20 percent nickel) can be effectively heat treated in a magnetic field of 10 oersteds if the temperature is above 400°C and below the Curie point of the alloy. The time during which the magnetic properties change has been measured at different temperatures and is found to vary according to the equation $\tau = Ae^{W/kT}$. The experiments are *interpreted* in terms of the domain theory of ferromagnetism. The changes which occur are due to the relief of magnetostrictive stresses which arise when the material becomes ferromagnetic upon cooling through the Curie point or when an external magnetic field is applied, and the relief comes about by plastic flow or diffusion in the separate domains. The values of A (about 10^{-12} second) and W (2.1 electron volts) are the same as those determined by Bragg and Williams for the above equation which also gives the time necessary for the establishment of a superstructure in alloys. The relation between the two processes, establishment of superstructure and the relief of magnetostrictive strains, is pointed out.

INTRODUCTION

PREVIOUS experiments[1] have established the fact that the magnetic permeabilities of some of the permalloys are considerably increased by heat treatment in a magnetic field of the order of 10 oersteds. The procedure is first to anneal the material in the usual way at about 1000°C and cool slowly, and then to apply a magnetic field to the specimen and maintain it while the specimen is reheated to about 500°C or higher and cooled again to room temperature.

The preceding paper describes an investigation of this phenomenon for a variety of iron-cobalt-nickel alloys, including especially the binary alloys of iron and nickel. The experiments described in the present paper have been done to examine in more detail the specific behavior of two interesting alloys, permalloy having 65 percent nickel and 35 percent iron (65 permalloy), and perminvar containing 20 percent iron, 60 percent cobalt and 20 percent nickel. They have to do mainly with the changes in magnetic properties that occur in the temperature range about 500°C. The results show that these changes in magnetic properties are to be associated with the relief of magnetostrictive strains by local rearrangement of the material. This will be discussed in more detail below.

[1] See the preceding article, this issue.

EXPERIMENTS WITH 65 PERMALLOY

An experiment showing particularly well the magnitude of the effect and the temperature range in which the application of the field is important, is illustrated in Fig. 1. Four specimens of 65 permalloy from the same casting were heated to 1000°C and cooled to room temperature, and in each specimen the magnetic field (10 oersteds) was applied during different temperature regions while cooling, as follows:

(1) Field applied during entire time of cooling.
(2) No field applied during entire cycle.
(3) Field applied only when cooling from 600° to 400°C.
(4) Field applied during cooling except from 600° to 400°C.

The effect upon the maximum permeability, as measured at room temperature after each cooling, is tabulated on Fig. 1. Application of the field as the specimen cools from 600°C (just above the Curie point) to 400°C, increases the maximum permeability from about 5000 to 250,000, or by a factor of 50.

To determine more definitely the temperature region in which the field is effective, the following series of runs was made on another single specimen[2] from the same lot of material. The annealed specimen was heated to 600°C and maintained

[2] The dimensions of this ring specimen were: 2.86 cm O.D., 2.38 cm I.D. and 0.63 cm axial height.

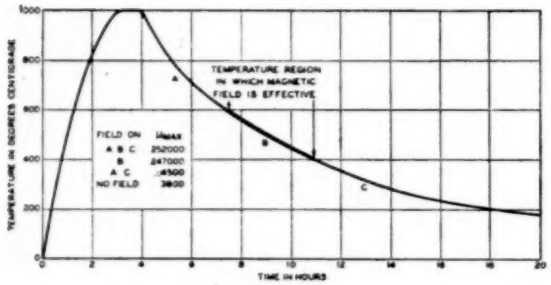

FIG. 1. Permalloy containing 65 percent Ni, originally hard worked, is heated and cooled as shown. The maximum permeability is increased about 50-fold if a field of 10 oersteds is applied in the temperature region indicated.

there for an hour, a field of 10 oersteds was then applied and the specimen cooled to a temperature t and maintained there for one hour. The field was then removed and at the same time the furnace began to cool to room temperature at the rate of about 150°C/hr. The maximum permeability μ_m was then determined and plotted against the temperature t as shown in Fig. 2, curve (a). A similar curve (b) was obtained by applying the same field at 600°C, but removing it as soon as the specimen arrived at the temperature t, no field being present either during the hour at temperature t or during the cooling to room temperature. The corresponding coercivity H_c is shown in curve (c). In the same figure the curve (d) shows the flux density B corresponding to a field strength of 10 oersteds, measured at the temperature t in a separate series of experiments. In order to obtain these data a second winding of deoxidized copper spaced from the first (H-producing) winding by two lavite rings was connected to the ballistic galvanometer (fluxmeter).

These experiments show that for heat treating this material in a field the effective range is from the Curie point down to a temperature of about 400°C. They do not show whether the effect is associated with the Curie point, lying, for example, in that range of temperature in which the magnetization changes most rapidly with temperature, or whether it occurs at the lowest temperature at which rearrangement (recrystallization or diffusion or plastic flow) takes place rapidly enough to be noticeable during the course of the experiments.

To settle this doubt we selected a second alloy, a perminvar, which was known to be affected by heat treatment in a field and which has a Curie

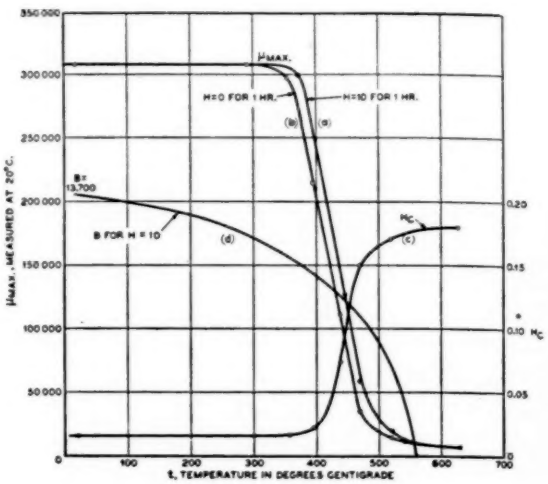

FIG. 2. Values of maximum permeability (curves a and b) and coercive force (curve c) of 65 permalloy measured at room temperature after heat treatment in a field. The field of 10 oersteds was removed at the temperature, t, on cooling. Curve d shows for comparison the value of B for $H=10$, measured at the temperature t.

point considerably higher than that of 65 permalloy.

EXPERIMENTS WITH PERMINVAR

The perminvar, selected for its high Curie point of 850°C, has the approximate composition 20 percent iron, 60 percent cobalt and 20 percent nickel. The first experiments, performed with 65 permalloy, were somewhat modified in the perminvar series. The specimen was heated to 950°C, 100° above the Curie point, and maintained there for one hour. The heating current in the furnace was then cut off and the material allowed to cool with the furnace, the cooling rate being approximately 200°/hr. at 900°C and 150°/hr. at 500°C. The magnetic field was applied at the temperature t, on cooling. The maximum permeabilities measured at room temperature are plotted as curve (a) of Fig. 3. Hysteresis loops were also traversed between ± 10 oersteds, and the discontinuous change in B, forming the vertical part of the side of such a loop, is plotted as curve (b) in the same figure. Curve (c) shows the value of B for $H=10$, measured at the temperature t.

In another series of experiments the specimen was heated for one hour as before at 950°C. Then the field of 10 oersteds was applied and cooling began. At the temperature, t, on cooling, the

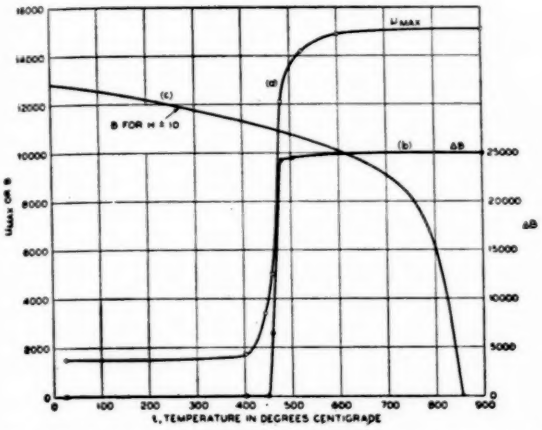

FIG. 3. Curve *a* shows the maximum permeabilities of a specimen containing 20 percent Fe, 60 percent Co and 20 percent Ni, measured at room temperature after cooling from 950°C, a magnetic field having been applied at the temperature, *t*, on cooling. Curve *b* indicates the change in *B* which occurs for constant *H*, the height of the vertical part of the hysteresis loop.

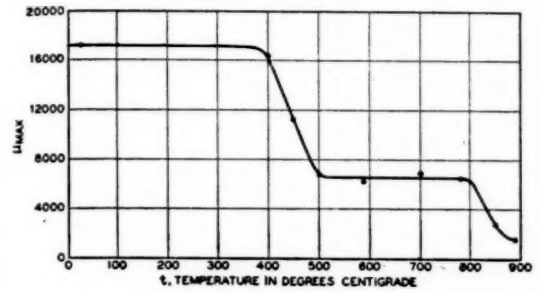

FIG. 4. Data similar to those of Fig. 3, except that here the magnetic field was applied during cooling from 950°C to temperature *t* and was then removed.

field was removed and remained zero till room temperature was reached. The maximum permeabilities, plotted against the temperature *t*, are shown in Fig. 4.[3]

In further experiments, measurements of relaxation time were made between 400° and 600°, the range in which magnetic changes occur as shown in Figs. 1 to 4. The specimen was heated to a temperature *t* and this temperature maintained constant within two or three degrees. At a recorded time a field of 10 oersteds was applied. At the end of one minute the field was reduced to zero and the galvanometer (fluxmeter) deflection read, after which the field was again applied and

[3] The highest values of μ_{max} in Figs. 3 and 4 are not the same; that for the latter is higher because it was measured after the specimen had been subjected to many more heating and cooling cycles and was therefore much more thoroughly annealed.

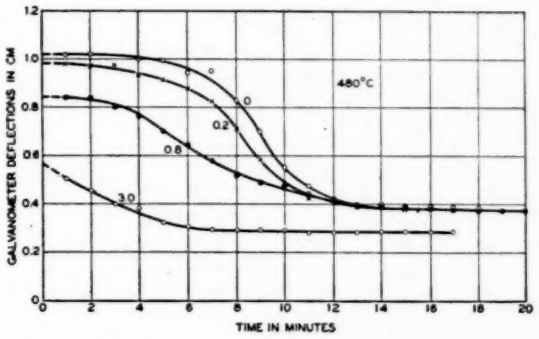

FIG. 5. Measurements made while the specimen (20 percent Fe, 60 percent Co, 20 percent Ni) was maintained at 480°C. A field $H=10$ was applied at zero time and held constant except for momentary changes, once each minute, to 0, 0.2, 0.8 or 3.0 oersted. The galvanometer deflections caused by these changes in *H* indicate changes in *B* and show how the magnetic properties change with time.

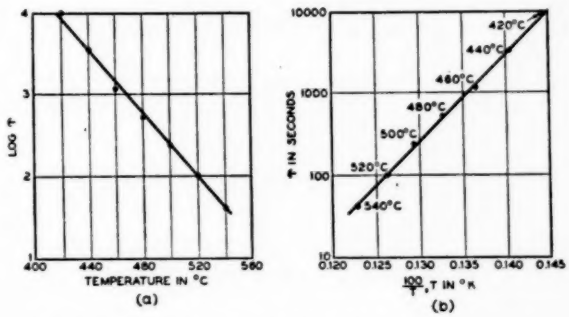

FIG. 6. The relaxation time, τ as dependent upon temperature.

the opposite deflection read. The average of the two deflections was recorded, and at the end of each minute thereafter similar observations were made. The total time during which the field was off was about five seconds per minute. The data for 480°C are shown in Fig. 5, curve "O." The last deflections here shown are due almost entirely to the air-flux, and were found to be nearly equal to the deflection for the same change of *H* when the specimen was above the Curie point.

We designate by τ the relaxation time, the time necessary for that part of the deflection which is to disappear, to change to $1/e$ of its original value. This relaxation time was determined for a series of temperatures, in this case always by changing *H* from +10 to +0.2, instead of from 10 to 0. Then log τ was plotted against the temperature *t*. The results are approximated by the straight line shown in Fig. 6(a). A plot of log τ against the reciprocal of the

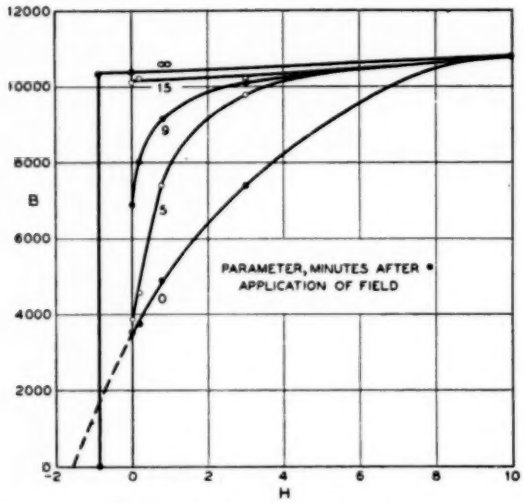

FIG. 7. Portions of the hysteresis loop measured at 480°C, at various times after the application of a field of 10 oersted.

absolute temperature T is also substantially a straight line as shown in Fig. 6(b).[4] This ambiguity results from the relatively small range in T.

Instead of changing H from 10 to 0 when taking ballistic deflections, in some experiments at 480° H was changed from 10 to either 3, 0.8 or 0.2 oersted. The corresponding deflections, shown by the curves of Fig. 5, were converted into flux density, B, and the latter plotted as a function of the time. Values of flux density and time from these curves were used in turn to plot parts of the hysteresis loops as they were at the times 0, 5, 9 and 15 minutes after the first application of the field of 10 oersteds. Fig. 7 shows these loops and the way in which they change gradually from the usual rounded form to the square form characteristic of material heat treated in a field.

DISCUSSION OF RESULTS

The results on 65 permalloy (Figs. 1 and 2) showed the heat treatment in a field to be effective when the field is applied in that range of temperature which is below the Curie point and above, say, 400°C. The results of Fig. 3 show that in spite of the higher Curie point this statement applies also to perminvar. For both materials the largest effects are produced when the field is present between 400° and 500°C, temperatures removed from the Curie point of the perminvar by 300° or 400°. It was thus established that the lower limit of 400° is independent of the Curie point, the only requirement being that the latter must be substantially higher than 400°C.

This lowest temperature at which the heat treatment is effective can be identified with that at which plastic flow begins to occur as the result of the forces brought into play by magnetostriction. These forces are of the order of magnitude of 0.1 to 1 kg/mm² as calculated from the magnetostrictive strain at saturation ($\approx 10^{-5}$) and Young's modulus ($\approx 2\times 10^4$ kg/mm²). There are as yet no data on the plastic flow of the alloys we have studied, but the data for nickel indicate that forces of this magnitude begin to produce flow at 400 to 500°C.[5] This point of view is borne out by Fig. 6, which shows that the relaxation time is an exponential function of the temperature, a relation known to hold for plastic flow.[6]

Another point is to be noticed in the curves of Fig. 7. A comparison of the curve for the initial time and that for five minutes shows that at the latter time the flux density for $H=0$ has changed very little (here $\tau=9.5$ minutes) whereas the flux-density for $H=3$ has changed 80 percent of the total amount it has to change ($\tau=3.0$ minutes). It is to be supposed that different parts of the specimen will be under strains of different magnitudes, and that during the annealing the largest strains will disappear more rapidly than the intermediate and smallest strains do. Since only the large strains affect the magnetic properties in high fields (e.g., $H=3$) the magnetization in high fields will change upon annealing before those in low fields ($H=0$).

The changes in magnetic properties of iron-nickel alloys due to cold working, and their recovery by annealing at various temperatures, have been studied by Tammann and Rocha.[7]

[4] In a paper on time lag in magnetization at high temperatures, Physik. Zeits. **32**, 860 (1931), H. Kühlewein has described slow changes in magnetization at 400°C and above, which he attributes to the slow relief of magnetostrictive stresses by plastic flow.

[5] Recent data of P. Chevenard, Rev. de Mét. **31**, 517 (1934), show that a stress of 1 kg/mm² will produce an extension of 10^{-5}/hr. at about 425°C. His data for iron indicate the corresponding temperature to be about 200°C higher than for nickel.

[6] Plastic flow due to magnetostrictive stresses has already been mentioned by Kühlewein (reference 3) and by H. Kersten, Zeits. f. Physik **71**, 560 (1931).

[7] G. Tammann and H. J. Rocha, Ann. d. Physik **16**, 861 (1933). In a series of papers, Tammann and his students

They find that complete recovery takes place only after annealing at 500° to 800°C, depending on the composition, but that the most rapid changes occur at 300° to 600°C. Analogous changes also occur for the electrical and mechanical properties. This range of temperature is roughly the same as that in which we observe the greatest magnetic effects due to annealing in a field, and the phenomena are undoubtedly very similar in nature.

Our data discussed above all support the plastic flow hypothesis provided we can show how plastic flow in the presence of a field increases the permeability in the direction of that field. In order to understand this, a more detailed consideration must be given to the changes which occur in the local strains, and their relation to the changes in magnetization. These considerations are given in the next section.

An additional remark should be made concerning Fig. 4. When the field is reduced to zero on cooling at any point between 700° and 500°C, the permeability at room temperature has a nearly constant value intermediate between the two extremes. We know of no good reason why this "shelf" should exist. According to the simple theory given below we should expect the permeability to be higher in this range.

Domain Theory of Heat Treatment

We start with the idea, as first proposed by Weiss many years ago and recently discussed anew by Webster, Heisenberg, Becker and others, that a magnetic material is composed of small domains, in each of which the material is magnetized to saturation in some direction. In iron and 65 permalloy this direction is one of the cubic axes of the crystals. In an unmagnetized polycrystalline specimen, in which the crystals are oriented at random, some domains are magnetized in every possible direction. As the field is applied in a certain direction, the magnetization in most of the various domains changes by 90° or 180° to become more closely aligned with the field. The sudden changes from one of the six directions of easy magnetization to another is the explanation of the Barkhausen effect.

Now consider what will happen to these regions as the material is heated above the magnetic transformation point. More specifically let us take, as shown in Fig. 8 (a) a region assumed spherical, for convenience, which is above the magnetic transformation point, but which will form a magnetized domain when cooled below this temperature. As shown in (b), it will become magnetized along one of the cubic axes; but as it does so it will tend to change its shape. If time is allowed, it may actually assume by plastic flow of its neighbors the ellipsoidal shape appropriate to magnetostriction, as shown in an exaggerated form in (c); or, it may do the equivalent thing and flow plastically within its own boundaries relieving the magnetostrictive stresses in this way. Then when the material is cooled to room temperature and is magnetized in the direction indicated in (d), the magnetization in this domain will reverse by 180° to one of its other stable positions more closely aligned with the field. No change in shape will occur during this change in magnetization. If, however, still at room temperature, we apply the field in the direction indicated in (e), the domain will *tend* to change its shape as shown by the dashes. But this change will be opposed by the mechanical constraints due to the surrounding material. If in another experiment the material is cooled rapidly enough through the magnetic transformation point down to a low temperature (<400°C), there will be in-

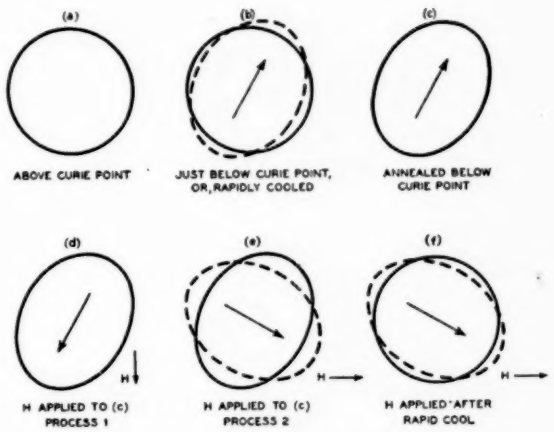

FIG. 8. Idealized domains (solid lines) under different conditions of heat treatment and magnetization. The dashed lines indicate in an exaggerated way the changes in shape which magnetostrictive forces tend to produce, and which do occur after plastic flow (or diffusion) of the material has taken place.

have reported also the recovery of various electrical and mechanical properties by annealing.

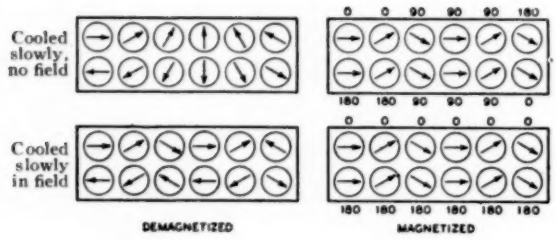
Cooled slowly, no field
Cooled slowly in field
0 0 90 90 90 180
180 180 90 90 90 0
0 0 0 0 0 0
180 180 180 180 180 180
DEMAGNETIZED
MAGNETIZED

FIG. 9. The changes in the direction of magnetization in domains, by 90° or 180° as indicated, upon application of a field.

sufficient time for any change in shape to occur by plastic deformation and the domain will maintain more or less its original spherical form. In such a condition (f) the magnetization of the domains may change by 90° or 180° with equal facility, whereas in slowly cooled material the domains can change by 180°C easily but by 90° only with great difficulty. This case can occur, for example, in 78 permalloy the permeability of which is higher after rapid cooling than after slow cooling: the additional probability of 90° rotations increases the number of domains which can easily be aligned with the applied field.

The effects of slow cooling both with and without a field, are illustrated in Fig. 9. Here in the first rectangle the domains are represented by circles and the directions of magnetization of the different domains are at random, as in an ordinary polycrystalline material. Actually in the figure all the directions of magnetization in a plane are shown in steps of 30°. When this material is magnetized as indicated the magnetization vectors will change by 0°, 90° or 180° to align themselves as nearly as possible with the field, consistent with the restriction that they must be magnetized in one of the easy directions of magnetization in the crystal, that is, along a cubic axis. Now when the material is annealed in a magnetic field, the domains will be oriented in the same ways but the strains produced by magnetostriction when it is cooled through the magnetic transformation point, will be relieved if the temperature and time allow (rectangle four). In steps of 30° in the two-dimensional model they will be oriented in just three ways. When the material is demagnetized at room temperature, these three positions will increase to six as shown in the third rectangle. When now it is magnetized again during measurement, each domain will change by 0° or 180°. Comparison of the second and fourth rectangles shows that when no field is present during heat treatment, half of the domains change by 90°, which they must do against the strong mechanical forces which oppose any change in shape, forces which are absent when the material is heat treated in a magnetic field.

These diagrams illustrate an additional point: If we try to magnetize this material at right angles to the direction in which the field was applied during heat treatment, each domain must change by 90° and very large mechanical forces will be operative resisting this change. This simple picture, then, indicates why the permeability should be higher after heat treatment in a field when the field is applied in one direction (parallel), and lower when it is applied in the other (perpendicular).

THE RELAXATION TIME

Within experimental error, the logarithm of the relaxation time is proportional to the reciprocal of the absolute temperature T, as shown in Fig. 6 (b); that is, $\tau = Ae^{W/kT}$, where $A = 2.8 \times 10^{-12}$ second, $W = 3.4 \times 10^{-12}$ erg (2.1 electron volts), and k is Boltzmann's constant. Or we may designate by T_1 the absolute temperature at which $\tau = 1$ second, and write

$$\tau = e^{-\ln A(T_1/T-1)},$$

where $T_1 = 931°\text{K}$ (658°C).

Equations of these forms have already been used by Bragg and Williams[8] to designate the relaxation time for certain properties of alloys which form superstructures. W is interpreted by them as the "activation energy" required for the interchange of atomic position which takes place during the formation or disruption of the superstructure, and for $AuCu_3$ has the value 2.0 electron volts. For the same alloy A has a value of about 10^{-12}.

Since the equation connecting τ with T is the same, both as to form and to the value of the constants, for the magnetic experiments described here and for the alloys with superstructure, it is important to consider what the two physical

[8] W. L. Bragg and E. J. Williams, Proc. Roy. Soc. A145, 699 (1934).

processes have in common. As pointed out by Bragg and Williams, the rate of interdiffusion of two metals is intimately connected with the relaxation times which they determine. But this rate is also intimately connected with plastic flow, especially one due to magnetostriction where there is deformation without change in volume. According to the simple theory described in the preceding section, during heat treatment either the boundaries of a domain are changed by plastic flow or the material inside adjusts itself to the unchanged boundaries. In a domain in which magnetostrictive stresses have just arisen, because of constrained boundaries, similar forces act upon each element of volume of the domain, and it is only necessary for readjustment of atom positions to occur within regions containing a few atoms for the whole domain to become stress-free. This readjustment is accomplished by diffusion, and it is to be expected that these relaxation times will be of the same order of magnitude as those for β-brass and for the gold-copper and iron-aluminum alloys discussed by Bragg and Williams.

We conclude, then, that both in alloys with superstructure and in ferromagnetic materials, we find the same mechanisms by which the changes take place and the same potential barriers to be overcome. The difference between the two phenomena is that in the one case the interatomic forces tend to put different kinds of atoms near together and in the other case the magnetic (magnetostrictive) forces act to change the distances between the atoms.

SEPTEMBER, 1935 PHYSICS VOLUME 6

A General Solution for the Displacements of Piezoelectric Media Which Are Subjected to Constant Electric Fields

ARNOLD D. HESTENES, *Department of Mathematics* AND HAROLD OSTERBERG, *Department of Physics, University of Wisconsin*

(Received June 7, 1935)

A general solution is presented for the displacements induced in any piezoelectric medium by static electric fields which are constant throughout the medium. This solution is then specialized to the case of α-quartz. The solutions for α-quartz have been used by the second writer in an accurate remeasurement of its piezoelectric moduli. The piezoelectric behavior of α-quartz is found to be closely predicted by these solutions.

I. THE GENERAL THEORY

ALTHOUGH the laws which govern the converse piezoelectric effect have for some time been described by Voigt[1] and Pockels,[2] general solutions for the corresponding displacements of piezoelectric media do not appear to have been developed. The solutions which are here presented apply to the case in which the piezoelectrically induced displacements are in equilibrium with electric fields which are constant throughout the medium. This is an important case.

Let the displacements u, v and w and the components of strain be defined as in Love.[3] It is convenient to write

$$\begin{aligned} e_1 &\equiv e_{xx}; & e_4 &\equiv e_{yz}; \\ e_2 &\equiv e_{yy}; & e_5 &\equiv e_{zx}; \\ e_3 &\equiv e_{zz}; & e_6 &\equiv e_{xy}. \end{aligned} \tag{1}$$

Let E_x, E_y and E_z represent the x, y and z components of the applied electric field intensities. The laws[1] which govern the converse piezoelectric effect may now be briefly written

$$e_i = K_i, \qquad i = 1, 2, 3 \cdots 6, \tag{2}$$

[1] W. Voigt, *Lehrbuch der Kristallphysik* (1910), p. 817.
[2] E. Pockels, Behandlungen der kgl. Ges. der Wissenschaften zu Göttingen 39 (1893).
[3] Love, *Mathematical Theory of Elasticity* (1920), pp. 35 and 38.

in which

$$K_i \equiv d_{1i}E_x + d_{2i}E_y + d_{3i}E_z. \tag{3}$$

The constants d_{ji}, $j=1, 2, 3$ and $i=1, 2, 3 \cdots 6$, are called the piezoelectric moduli. For a given applied electric field K_i are constants since these fields are assumed to be independent of the time and the coordinates x, y and z.

From (1) $e_1=\partial u/\partial x=K_1$; $e_2=\partial v/\partial y=K_2$; $e_3=\partial w/\partial z=K_3$. Hence,

$$\begin{aligned} u &= K_1x + f_1(y, z) + L_1, \\ v &= f_2(x, z) + K_2y + L_2, \\ w &= f_3(x, y) + K_3z + L_3, \end{aligned} \tag{4}$$

in which f_i are undetermined functions and L_i are constants.

$$\begin{aligned} & e_4 = \partial v/\partial z + \partial w/\partial y = K_4. \\ \therefore \quad & \partial f_2(x, z)/\partial z + \partial f_3(xy)/\partial y = K_4. \end{aligned} \tag{5}$$

If $f_2(xz)$ is not linear in z alone, $\partial f_2(xz)/\partial z = F_2(xz)$. If $f_3(xy)$ is not linear in y alone, $\partial f_3(xy)/\partial y = F_3(xy)$. Since x, y and z are independent variables, it follows that the sum of $F_2(xz)$ and $F_3(xy)$ cannot be equal to a given constant K_4 for all values of x, y and z. This consideration is sufficient to show that $f_2(xz)$ is linear in z alone and that $f_3(xy)$ is linear in y alone since the alternative that f_2 and f_3 are both independent of x leads to the trivial case in which f_i are constants when the consequences of $e_5=K_5$ and $e_6=K_6$ are similarly analyzed.

Upon expanding $e_5=K_5$ and $e_6=K_6$ in a manner similar to $e_4=K_4$ above, it is found that

$f_1(yz)$ is linear in y alone and in z alone;
$f_2(xz)$ is linear in x alone and in z alone;
$f_3(xy)$ is linear in x alone and in y alone.

From the above considerations Eqs. (4) may be written

$$\begin{aligned} u &= K_1x + b_1yz + c_1y + h_1z + k_1, \\ v &= a_2x + b_2xz + K_2y + h_2z + k_2, \\ w &= a_3x + b_3xy + c_3y + K_3z + k_3, \end{aligned} \tag{6}$$

in which a_i, b_i, c_i, h_i and k_i are constants. When Eqs. (6) are substituted into $e_i=K_i$ ($i=4$, 5 and 6), it is found that

$$b_1=b_2=b_3=0; \tag{7}$$
$$h_2+c_3=K_4; \tag{8}$$
$$h_1+a_3=K_5; \tag{9}$$
$$c_1+a_2=K_6. \tag{10}$$

Since $b_i=0$, u, v and w do not contain cross product terms of the Cartesian coordinates.

When (7), (8), (9) and (10) are substituted into (6),

$$\begin{aligned} u &= K_1x + (K_6-a_2)y + h_1z + k_1; \\ v &= a_2x + K_2y + (K_4-c_3)z + k_2; \\ w &= (K_5-h_1)x + c_3y + K_3z + k_3. \end{aligned} \tag{11}$$

The constants a_2, c_3, h_1, k_1, k_2 and k_3 depend upon the boundary conditions, i.e., upon the manner in which the piezoelectric plate is supported. If the origin of the Cartesian coordinates is chosen at some point at the fixed support, u, v and $w=0$ at this point. Therefore $k_1=k_2=k_3=0$. Since it is usually possible to select the origin in this manner, then quite generally

$$\begin{aligned} u &= K_1x + (K_6-a_2)y + h_1z; \\ v &= a_2x + K_2y + (K_4-c_3)z; \\ w &= (K_5-h_1)x + c_3y + K_3z. \end{aligned} \tag{12}$$

When the remaining constants a_2, c_3 and h_1 have been properly determined from the boundary conditions, Eqs. (12), (2) and (3) determine the displacements which are brought about by a constant electric field in any piezoelectric plate.

II. Application to α-Quartz

In α-quartz[4]

$$\begin{aligned} K_1 &= d_{11}E_x; & K_4 &= d_{14}E_x; \\ K_2 &= -d_{11}E_x; & K_5 &= -d_{14}E_y; \\ K_3 &= 0; & K_6 &= -2d_{11}E_y. \end{aligned} \tag{13}$$

Eq. (12) reduces to

$$\begin{aligned} u &= xd_{11}E_x - (2d_{11}E_y + a_2)y + h_1z, \\ v &= a_2x - yd_{11}E_x + (d_{14}E_x - c_3)z, \\ w &= -(d_{14}E_y + h_1)x + c_3y. \end{aligned} \tag{14}$$

Various important cases arise, depending upon the manner in which the quartz plate is mounted and upon the direction along which the electric field is applied.

Case A: *$E_y=0$ and the crystal plate so mounted that $v=0$ when $y=0$ and the plane $y=0$ suffers no rotation about Y.*

Since $v=0$ when $y=0$, $a_2=0$ and $c_3=d_{14}E_x$.

[4] W. Voigt, *Lehrbuch der Kristallphysik* (1910), p. 830.

Since there shall be no rotation of the plane $y=0$ about Y, $h_1=0$. Hence,

$$u=xd_{11}E_x; \qquad v=-yd_{11}E_x; \qquad w=yd_{14}E_x. \quad (15)$$

This case is approximated when the usual rectangular X cut is allowed to rest upon a Y face and the field is applied through electrodes which cover the X faces. The origin is chosen at the center of the Y face upon which the plate is allowed to rest.

Eq. (15) is found to hold also when the X cut is mounted such that $u=0$ when $x=0$ and that $v=0$ for all values of z in the plane $x=0$. This latter case is closely approximated when the plate is allowed to rest under the action of gravity upon an X face and when the origin is chosen at the center of this face.

Case B: *$E_y=0$ and the crystal so mounted that $w=0$ when $z=0$ and the plane $z=0$ suffers no rotation about Z.*

Since $w=0$ when $z=0$, $c_3=h_1=0$. Since there shall be no rotation of the plane $z=0$ about Z, $a_2=0$. Hence,

$$u=xd_{11}E_x; \quad v=-yd_{11}E_x+zd_{14}E_x; \quad w=0. \quad (16)$$

This case is closely approximated when the rectangular X cut is allowed to rest under the action of gravity upon a Z face at the center of which is located the origin of the Cartesian coordinates.

A comparison of (15) and (16) emphasizes the fact that the displacements u, v and w depend markedly upon the method of mounting the X cut. The correctness of Eqs. (15) and (16) has been verified by experimental tests which have been made at this university. These experiments will be described elsewhere.

Case C: *$E_x=0$ and the crystal so mounted that $v=0$ when $y=0$ and there is no rotation of the plane $y=0$ about Y.*

Since $v=0$ when $y=0$, $a_2=c_3=0$. Since there is no rotation about Y, $h_1=0$. Therefore

$$u=-2yd_{11}E_y; \qquad v=0; \qquad w=-xd_{14}E_y. \quad (17)$$

This case is closely approximated when the usual rectangular X cut of α-quartz is allowed to rest under the action of gravity upon a Y face at the center of which is chosen the origin.

Cases A, B and C constitute three of the most important cases which arise in connection with rectangular plates of α-quartz. They illustrate the manner in which a_2, h_1 and c_3 of Eq. (12) or (14) may be determined from the boundary conditions.

Eq. (14) has been applied by the second writer to the measurement of the piezoelectric moduli d_{11} and d_{14} in α-quartz. These measurements have in every case substantiated the validity of (14) and therefore of the phenomenological theory of piezoelectricity.

On Anchoring the Mercury Pool Cathode Spot

LEWI TONKS, *Research Laboratory, General Electric Company*

(Received March 20, 1935)

Certain metals projecting through a mercury surface are known to have the property of "anchoring" the cathode spot. A variety of metals have been examined for this ability and it has been found to exist for all of them tried, Fe, Pd, Zr, Pt, Cr, Cb, Ir, Mo, Ta, W. The property depends upon wetting of the metal by the mercury, and this in turn depends upon having a clean metallic surface. The spot lengthens into a fine bright cathode line (C.L.) at the meniscus edge. These metals differ in the ease of cleaning and of maintaining cleanliness. Electrolysis, hydrogen firing, vacuum firing and ion bombardment were used in different cases. The first five show attack by the cathode spot, the Mo shows slight disintegration. Besides the bright line spectrum, the C.L. has also a strong, continuous spectrum from red into ultraviolet which is quite different from hot body radiation. The C.L. consists of a multitude of small emitting areas which are in constant rapid and chaotic motion. The details as shown by moving film photographs differed with the anchor. Cb showed the most clear-cut phenomena. Its individual spots passed 0.22 amp. each and they moved with a predominant velocity of 46 cm/sec. They oscillated in intensity with a period of the order of 10^{-4} sec. Their current density was ~9000 amp./cm². The behavior of the C.L. under different kinds of varying current has been observed, and the change in C.L. length with current plotted. Increasing the arc current while maintaining the length of C.L. fixed resulted in a lowering of the C.L. even to below the pool level and to the formation of a trough in the liquid outside the C.L. This helps explain the mechanism of spot freeing at large current densities and gave the upper limit for a circular anchored spot at about 40 amp./cm.

IT HAS been noticed that certain metals projecting through the surface of a mercury pool cathode hold the cathode spot and prevent its wandering over the pool. As far back as 1903 E. Weintraub of this laboratory noted the effect with platinum and platinum-iridium wires. In 1931 S. Sweetser observed similar behavior with a molybdenum wire. More recently there have been references in the literature[1] to anchoring the cathode spot in this way by using W or Mo as the anchor.

A cathode spot may dodge about the surface of a pool for minutes, setting up vigorous wave motion, throwing spray about erratically, and causing the incessant flickering of positive glow in short tubes, or an unsteadiness of the lower end of the positive column in long tubes. Measurements have shown large pressure fluctuations some distance from the cathode.[2] Occasionally the spot may hover at an Mo surface projecting through the mercury. It sometimes plays over the Mo surface itself, as if, perhaps, following a droplet which it is chasing. Suddenly the spot will settle down as a ball of blue-white glow at the junction between mercury and Mo, and the general wave motion will disappear leaving only a set of standing waves directly before the spot to bear testimony to a pressure originating in it. Gradually the spot lengthens into a fine luminous blue-white line which is seen to lie along the junction between mercury and molybdenum, and the surface of the mercury is quiet. The spray has ceased, the flickering often stops entirely. The arc drop becomes steadier, or even constant, within the range of the former fluctuations. Everything indicates that we are now dealing with a far steadier process than before.

Examination of the mercury molybdenum junction shows that the mercury is wetting the Mo over the length occupied by the anchored spot, which is more appropriately called a *cathode line*. If the current in the arc is suddenly increased, the C.L. (cathode line) brightens and the mercury before it becomes agitated. Gradually the line lengthens out as the Mo bordering it becomes clean and wet by the action of the discharge. In this way it has been possible to increase the carrying capacity of an anchored spot from 5 to over 90 amperes. But unless cooling provisions are adequate, the spot frees itself shortly.

When a comparatively small current was drawn from a metal-Hg junction which had been well wet by a large current, a distinct unsteadiness in the anchored spot itself became evident,

[1] Ludwig and Maxfield, Elect. Eng. (1) **53**, 74 (1934); Kömmnick and Lübcke, Physik. Zeits. **33**, 215 (1932).

[2] Unpublished work by K. H. Kingdon and E. J. Lawton.

and the line possessed a marked mobility along the meniscus edge. This did not occur when larger currents had not been drawn, for then the Mo was not wet beyond the limits of the line. Examination of the C.L. on Mo with a magnifying glass revealed a rapid and erratic, though minute, vertical motion in the line.

Many questions regarding this phenomenon present themselves, but in what follows three in particular will be dealt with: First, what metals will anchor the spot, second, what the general nature of the C.L. is, and third, the effect of restricting the length of line to small values.

Anchoring Properties of Various Metals

The tests on the anchoring quality of various metals were rough and intended to give a general rapid survey rather than complete and accurate information. They were made with an arc tube of the form shown in Fig. 1. *A* and *B* were two graphite anodes, and *P* was the pool cathode whose level could be adjusted by means of the barometric column. *S* was the sample under test, preferably in the form of a strip bent into a *U* whose ends were welded to the two leads of a stem which formed a ground glass joint with the tube proper. This joint was made vacuum tight with sealing wax.

The strip *S* could be given a preliminary cleaning treatment in air, and could then be heated to high temperature in vacuum for further cleaning by passing current through it. It could also be subjected to ion bombardment from the arc between *P*, in a lowered position, and *A*. Samples which could not be worked into sheets were welded to one of the leads and by using them as anode they could be heated to high temperatures.

The anodes *A* and *B* were always degassed by drawing large currents to them before tests were made on *S*. During this operation *P* lay below *S*, so that *S* was immersed in the plasma. *S* was insulated so that it was approximately at cathode potential.

The behavior of the various metals tested can be summarized as follows: Ir, Pt and Pd became uniformly wet and anchored well with no or little heating. Mo, hydrogen fired, anchored after short exposure to the cathode spot. Cb and Cr

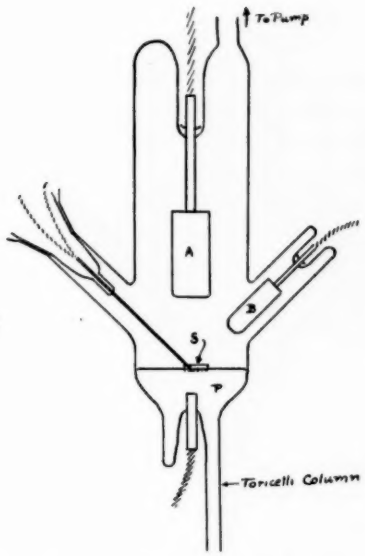

Fig. 1. Mercury arc tube for anchoring tests.

only anchored well after ion bombardment. Zr was wet by raising the Hg over it while it was hot. W was wet in the same way or by ion bombardment. All of these metals held the cathode spot well once it had anchored. Fe, though not difficult to wet, anchored poorly. With Ta drastic treatment was necessary to obtain anchoring, and then the condition was only temporary.

Another effect developed in connection with this phenomenon. A metallic deposit appeared on the glass wall opposite the C.L. on certain of the metals. This consisted of material transferred from the anchor, the erosion of the latter being visible after removal from the anchor tube. This behavior was characteristic of the metals having a melting point below 1900°C. A very much slower attack has been noted on Mo. The eroded material appeared as a fine powder floating on the pool.

Before the slight disintegration of Mo had been found, the apparent immunity of the more refractory metals suggested that a temperature of about 1900°C might exist at the anchored spot even though many considerations point to temperatures under 200°C in the free spot.

Spectrograms of a C.L. were taken with both a glass and quartz spectrograph, and strong continuous radiation was found extending from the red to the limit of the quartz instrument—about 2300A. An optical pyrometer with a red

filter gave an apparent temperature of 1050°C for the C.L. Comparison of the spectrum of an Mo strip heated to this temperature, as judged by the pyrometer, with that of the C.L. showed that the latter had an intensity distribution entirely different from that of a hot body, the short wavelength energies (extending into the ultraviolet) being too great. This is in rough agreement with Lübcke[3] who found increasing apparent temperature as he went from red to blue for his color matches. The present measurements indicate a far higher "temperature" in the blue than the 1295°C which he found and probably approach more nearly to the 2087°[3] which has been reported in the green.

The anomalous intensity distribution in the continuous spectrum shows that this radiation does not originate in a high temperature of the anchor. It is probably due to transitions between hyperbolic orbits[4] in the highly ionized gas close to the electron emitting surface. Clearly this case is different from that of the copper cathode of the copper arc,[5] where rough agreement between pyrometer temperature and temperature calculated from the copper evaporation has been found, for here the mercury temperature must be but a fraction of the optical "temperature." It is interesting, however, that in both cases the experiments lead to the concept of a small region of "hot" gas close to the cathode surface. Parenthetically, the spectrograms also show great broadening of the spectrum lines in the C.L., which is attributable to Stark effect due, probably, both to high ion concentration in the cathode spot plasma and to high field strength in the cathode sheath.

As remaining possible explanations for the cathodic attack there is either (1) solution by the Hg at the temperature, probably of the order of 150°C, at the cathode spot, or (2) new disintegration effects arising from the extremely high concentration of the 10-v ions which bombard the cathode. As to the former there is too little solubility data by which to check, and, in either case, the correlation with melting point remains unexplained.

[3] E. Lübcke, Zeits. f. tech. Physik (12) **10**, 598 (1929).
[4] W. Finkelnburg, Phys. Rev. **45**, 341 (1934); Zeits. f. Physik **88**, 297, 768 (1934).
[5] R. Tanberg and W. E. Berkey, Phys. Rev. **38**, 296 (1931).

General Nature of the Cathode Line

A rotating mirror viewing of a C.L. showed, not the uniform luminous band that would have resulted from a continuous line of light, but a mottled strip which could only arise from rapid point-to-point variations.

A camera was built to photograph the image of the C.L. on a moving film. Light from the C.L. leaving the meniscus edge at an angle slightly above the horizontal so that the Hg pool should not cut off needed light was focused by a camera objective onto the film mounted on the rotating drum of an oscillograph film holder. The objective, an f4.5, 10.5 cm focal length lens was used camera side toward the C.L. because it was enlarging. A simple shutter just in front of the film holder was arranged to be opened and closed for the approximately 1/10 second duration of exposure by the back-and-forth motion of a hand-operated lever. The film drum was driven by an 1800 r.p.m. synchronous motor through a reducing gear ratio of 102 to 36. As the exposed length of film was 31.45 cm, it follows that the linear film speed was 333 cm/sec. The magnification was found to be 2.62 by photographing cross-section paper in the position of the cathode line.

Fig. 2 shows two traces of a C.L. anchored to a strip of columbium, the upper being of a 1 amp., the lower of an 8-amp. line. The fading out along the lower edge of the latter was caused by an obstruction in the camera. The occasional localized fogging arises from a temporary concentration of emitting points. This condition is directly observable when the anchor is poorly wet so that the C.L. cannot expand freely, often occurring, as already mentioned, when the spot first anchors. The electron density or the vapor density, or both, just beyond the C.L. become great enough to cause the brilliant glow which extends 1 mm or more into space and is responsible for the fogging. This glow obliterates the C.L. for the unaided eye, but an interposed ruby glass reveals it.

These traces reveal much concerning the C.L. First is the fact that the "line" consists of a multitude of rapidly moving points. The motion of any one point is frequently uniform for a considerable distance. These points are seemingly independent of each other, yet as a whole they cling together as shown by the fact that the 1-

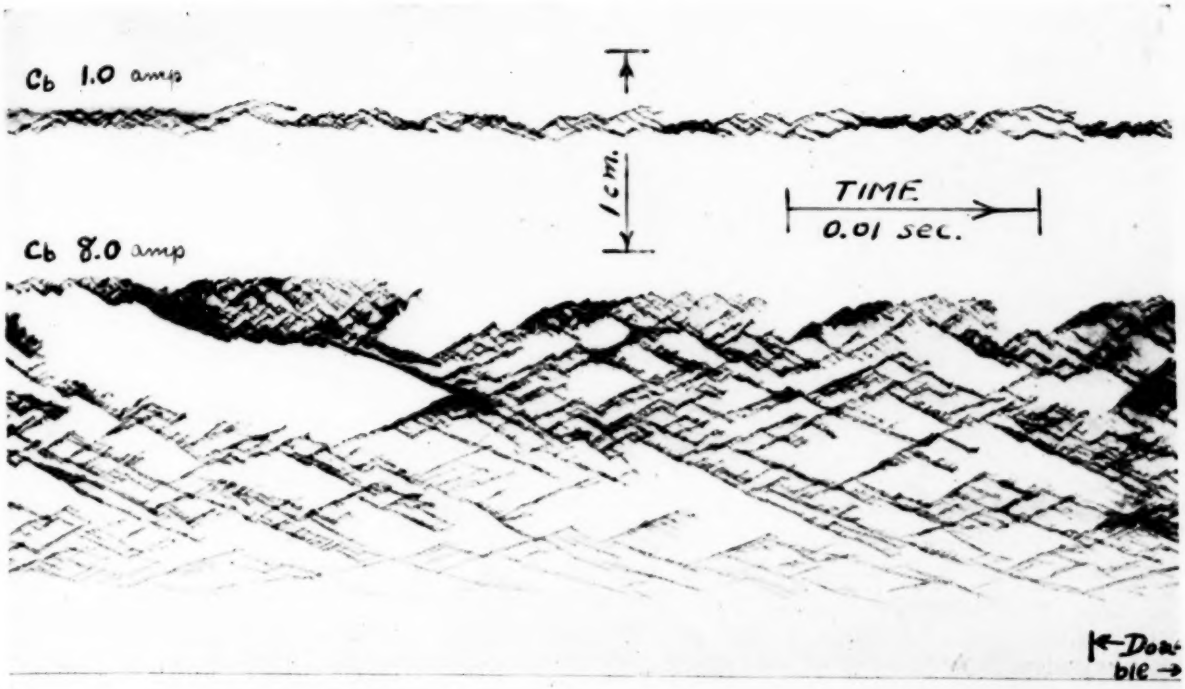

FIG. 2. Moving film trace of cathode line on columbium, constant current. Full size reproduction of film, space dimension referring to C.L. itself.

amp. line occupies only a small portion of the available meniscus edge. In some way the greater overall width of the 8-amp. trace made it possible for individual emitting points to traverse greater distances at approximately constant velocity.

Measurements on a trace not reproduced here showed the predominating single spot velocity to be 46 cm/sec., although velocities as high as 146 cm/sec. were found.

Each spot track has a beaded appearance, which, although clear on the film, may not reproduce in the figures. It is as if the spot oscillated in intensity with a period of about 0.5 to 1.5×10^{-4} sec. This may show an essential instability. An accurate determination of this frequency has not been attempted as yet.

Due, possibly, to this instability spots are continually both dying out and splitting in two, each of the pair to continue independently, one usually in the original direction with the original speed, the other in the opposite direction. Oftentimes the second spot is short lived. In some cases it disappears so soon that it is impossible to say whether it is a new spot or just a strong bead.

Rough counts of the number of tracks encountered in passing from one side of a trace to another indicated that the number of spots in the C.L. is proportional to the current. Accurate determinations of the amperes per spot were not possible at the larger currents because the frequent splitting and dying out of spots made counts indefinite. At lower currents places on the traces could be found where this difficulty was a minimum. Four such tracks gave the values with probable errors shown in Table I. Although the current range is small, being limited at the lower end by the tendency of the spot to extinguish, the values vary far less than the current. In view of the phenomenon as a whole, it seems practically

TABLE I. *Spot counts on Cb traces.*

Trace	Current (amp.)	No. of tracks, ave.	Percent deviation, ave.	Amp. per spot
9a	1.5	6.8	7.5	0.221
9b	1.5	6.8	7.5	0.221
11a	1.0	4.7	12.5	0.213
11a-b	1.3	5.75	6.5	0.226
7a	1.0	4.44	9.0	0.226
				Average 0.221

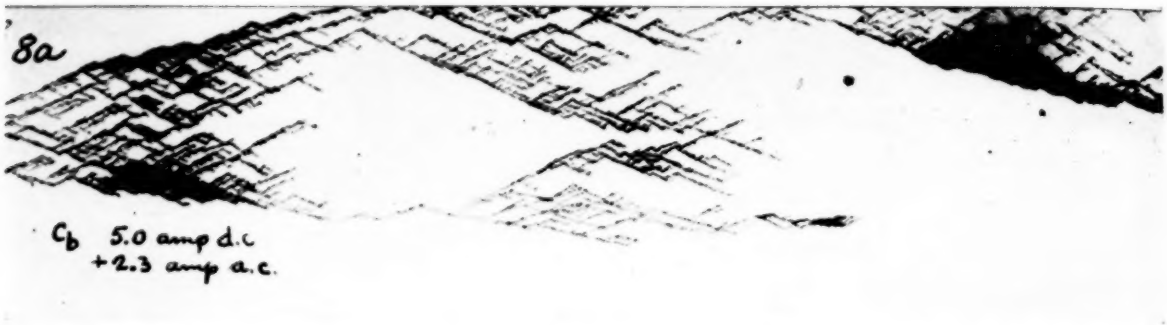

FIG. 3. Columbium cathode line passing sinusoidally varying current. Full size reproduction of original film.

certain that the relation 0.22 amp./spot was maintained at all currents.

The beads themselves are very small. Examination of the oscillograph films under low magnification has shown them to have indefinite boundaries, and to vary in their dimension along the C.L. (i.e., perpendicular to the trace) in the ratio of four to one. It is quite possible that the image size is at least partially due to the limited resolution of the lens, or to distortion by the cylindrical tube walls. This was not checked with the apparatus used because it is intended to make further photographic studies under more carefully controlled conditions. We can, however, determine an upper limit to the range of bead sizes. The photographs do not distinguish between extension along and extension perpendicular to the meniscus edge, but whichever dimension of the image is greater is again an upper limit to the maximum bead dimension. The larger bead images measured 0.02 cm across in both directions. Reducing this by the magnification, 2.62 in that case, gives a bead diameter of 0.008 cm. Assuming a circular spot, the area is 5×10^{-5} cm². Because of the oscillations, the current flowing from the bead is probably more nearly 0.44 amp. than the 0.22 average. This gives a current density of 9000 amp./cm² in the individual spot at maximum. Values which have been determined for the free spot on mercury are 4000 amp./cm² by Güntherschulze[6] and 1912 amp./cm² by Kobel.[7]

Parenthetically, I have examined some moving film pictures of the free cathode spot taken by I. Langmuir and K. Blodgett some years ago. They were not very satisfactory for measurement because they were made with a reducing lens system, and the grain structure of the film sets a limit to the definition. Nevertheless, it is clear that the area of the cathode spot image varies several fold with time and even disappears occasionally to reappear an instant later. This can only mean that the depression made by the spot extends obliquely downward so that its sides become interposed in the light path. This would also account for apparent variable spot area. The measurements which I have made on these films give values of current density ranging from 3000 to 18,000 amp./cm².

Cathode line arc tubes have been tried in three different circuits in order to observe the behavior of the line under different types of current demand. Fig. 3 shows the C.L. behavior when a.c. was superimposed on d.c., giving a sinusoidal current variation between 1.75 amp. minimum and 8.25 amp. maximum. The behavior in successive cycles was not uniform, little fog appearing in one of them, no fog in another, and a great deal in the third. But nothing essentially new is brought out. The emitting point velocities were the same.

As another test a thyratron circuit was used which made an instantaneous demand for current in addition to that used for holding the arc. Fig. 4 shows that an increase from 1.5 to 5.0 amp. was accomplished almost without causing additional glow near the C.L. and with very little immediate expansion of the C.L. But an 8-fold multiplication from 1.5 to 11.5 amp. caused an instantane-

[6] Güntherschulze, Zeits. f. Physik **11**, 74 (1922).

[7] Kobel, Phys. Rev. **36**, 1636 (1930). This author measured the current flowing from a small limited free surface of Hg when it was completely covered by the cathode spot. How to judge when this condition is reached is not at all obvious, and may, in fact, be difficult. It appears highly likely that one-third to half of the current originated in a C.L. on the tungsten wall. Altogether this value of current density is extremely doubtful.

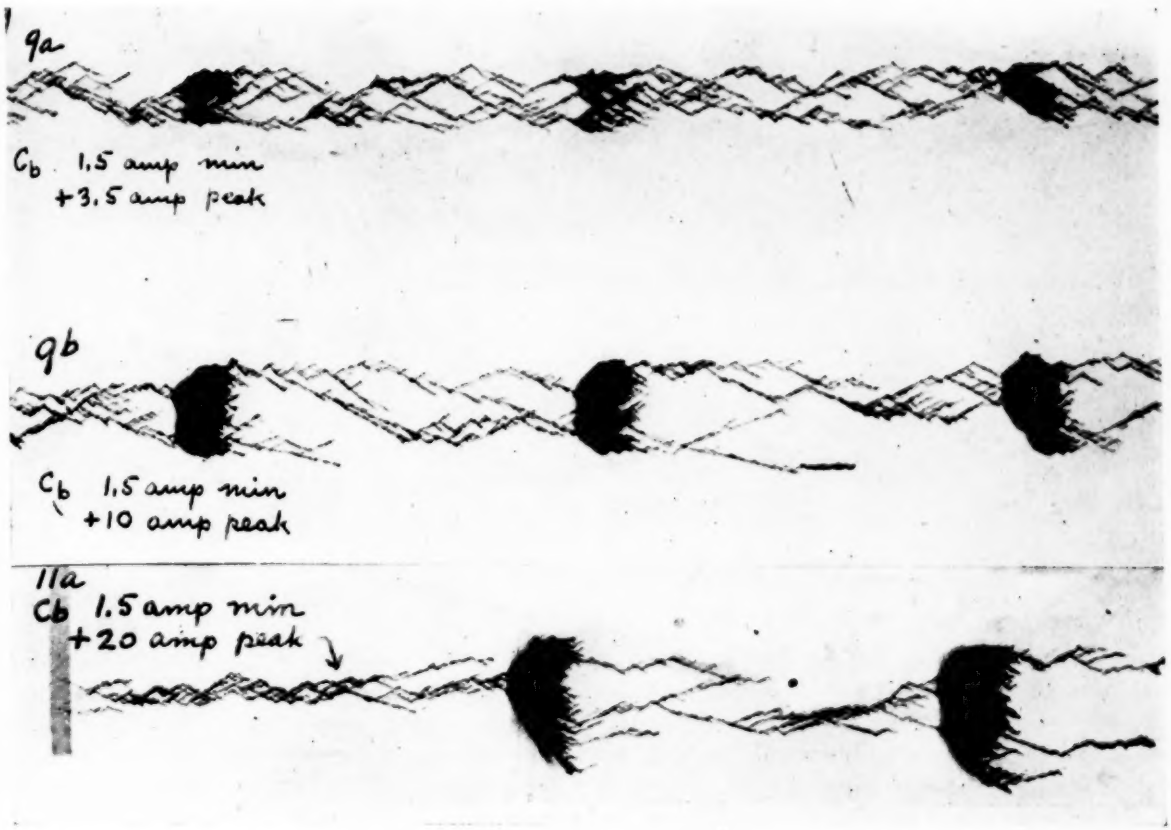

FIG. 4. Columbium cathode line passing saw-tooth current pulses from thyratron circuit. Full size reproduction.

ous lengthening of the C.L. and created an intense glow due to momentary crowding of the newly-born emitting points. These effects were even more pronounced when the increase was to 21 amp. Direct observation of the line showed, however, that there was no freeing of the spot even under this condition.

As a third test 40 μf charged to 125 v in series with about 0.25 ω was discharged through the tube. The traces, of which Fig. 5 is typical, showed an instantaneous spreading of the C.L. accompanied by a general glow in the tube. There followed a few oscillatory discharges, then a quiescent period, and finally sustained oscillations until the condenser circuit switch opened.

The quiescent period may be caused by the transitory abnormal vapor density in the tube, the first few oscillations occurring before the density has increased. The few milliseconds of this first period seem to be longer than would be required for the vapor to spread throughout the tube from the cathode spot. Possibly the density increase comes from the evaporation of fine spray thrown against the hot tube walls or anode by a momentary partial freeing of the spot during the condenser discharge.

The relaxation oscillations of Fig. 6 are to be contrasted with those in Fig. 5 where with a smaller current flowing, the condenser discharge occurred in general through one and sometimes two enhanced spots. In Fig. 6, however, the spots number four and five, are well separated, and are regularly spaced on the film by virtue of the equal timing of discharges and the uniform velocity of the spots. This, too, results in enhanced spots lying at the confluence of two tracks, so that not only do a pair of tracks frequently leave an enhanced spot, but about as frequently, two tracks enter one.

Traces with the same circuits, as used with the Cb anchor, were made using Mo. Nothing distinctive was observed insofar as the response to the current demand was concerned.

But the Mo trace itself differs markedly in

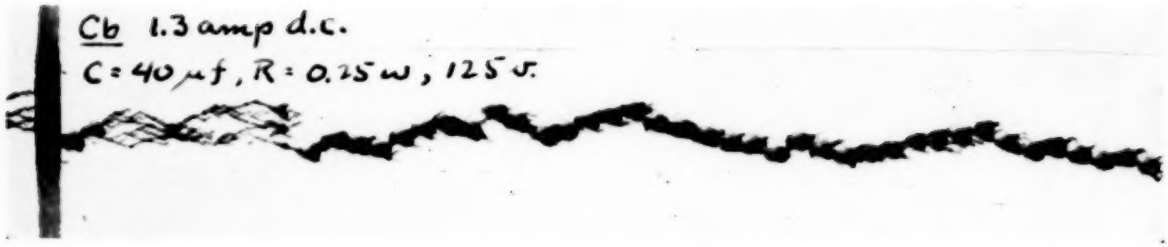

FIG. 5. Columbium cathode line carrying condenser discharge. Full size reproduction.

FIG. 6. Columbium cathode line carrying relaxation oscillations. Full size reproduction.

structure from Cb. Fig. 7 shows the trace for Mo with a trace of Al added to the mercury to aid anchoring. Comparison with pure mercury traces has shown no significant difference. The C.L. in Fig. 7, instead of consisting at any instant of a set of discrete emitting points, appears to be made up of a smaller number of short emitting line lengths which themselves show an uneven distribution of light, and hence probably emission, over their lengths.

Undoubtedly the vertical motion in the C.L. confuses the picture. In this connection, it is possible that the horizontal motion of emitting areas is not as free along Mo as along Cb, so that the local cathode spot force depresses the meniscus edge over a very short distance until either the local spot is extinguished or moves laterally to a new position. Examination of the Mo traces reveals apparent gaps in the tracks, but the originals show very faint connecting links, so that these gaps constitute instances of extreme spot variability.

Regarding the other traces in Fig. 7, the Ir shows a fairly definite fine structure. In the case of W(Al) it was possible to make a rough count of tracks. The value found was 0.39 amp./spot with an average deviation of 16 percent.

In all three cases, a group of emitting spots, the elements of which were moving rapidly with respect to each other, traveled as a whole for considerable distances with approximately constant velocity. W(Al) furnished the outstanding example in the 5-amp. trace, where the uniform progress was interrupted only to be resumed a moment later. This behavior was undoubtedly due to waves in the mercury traveling lengthwise of the anchor. If a particular level of the anchor was especially favorable for the maintenance of the spot, a traveling wave would cause just such an effect.

Although the length of C.L. was far from being constant under constant conditions, that it increased with increase in current was unmistakable. Frequently the overall width included large momentary gaps, but no reasonable criterion could be set up to judge when such a space should be included within the C.L. and when it should be excluded. Accordingly, in measuring trace width (i.e., C.L. length) the overall width between extreme emitting points was always taken, no matter how wide or persistent the gaps. Measurements were made at a series of equal spaced positions along each trace.

The average C.L. lengths for the 18 traces measured are shown in Fig. 8 plotted against arc current. The nature of the anchor is designated as indicated in the figure. The single Mo(Al) point is that at 1.3 amp. The average deviation of the individual measurements from the plotted average is shown by the vertical line segment through

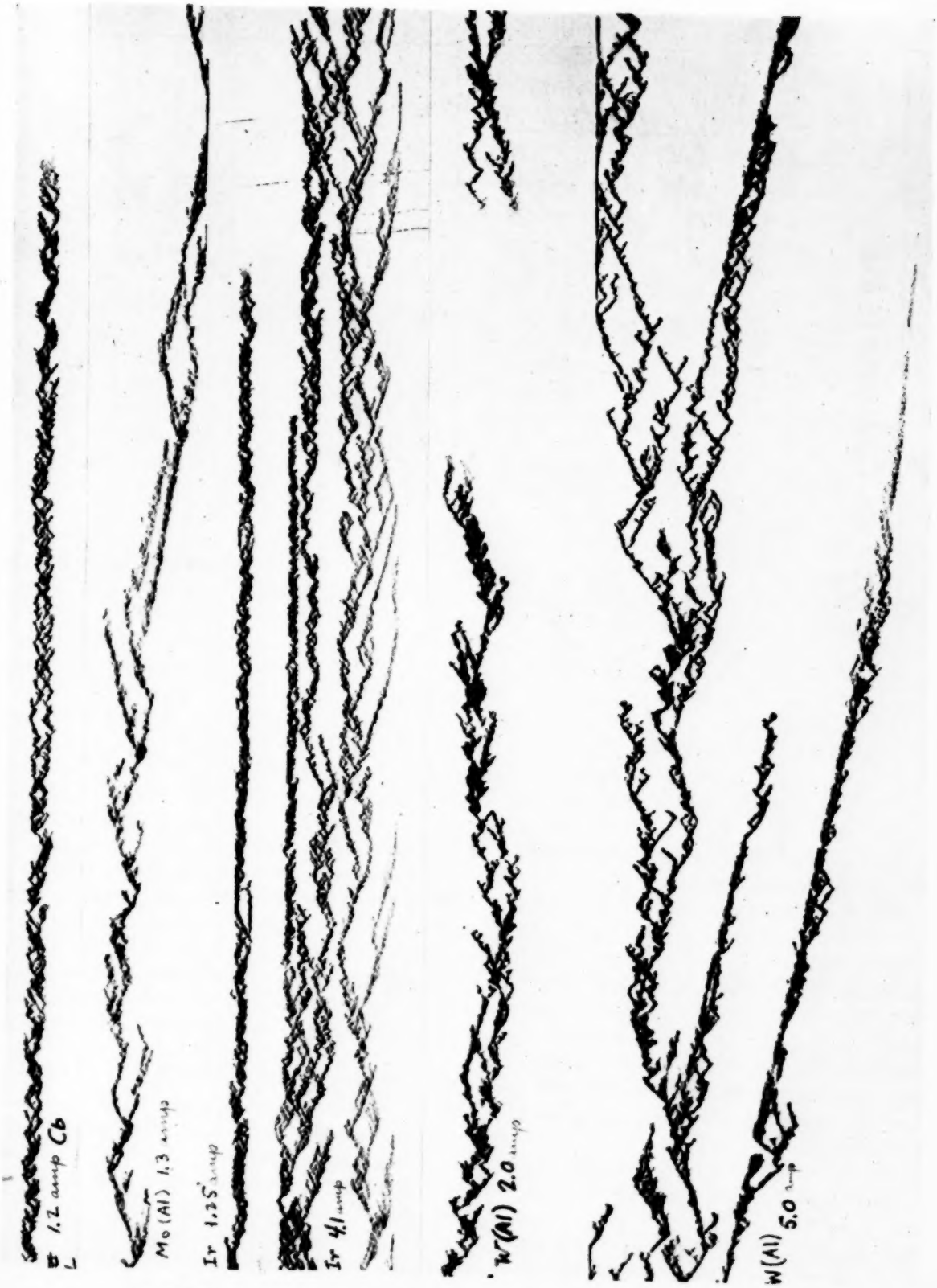

FIG. 7. Cb, Mo(Al), Ir, W(Al) cathode line traces. Full size reproduction.

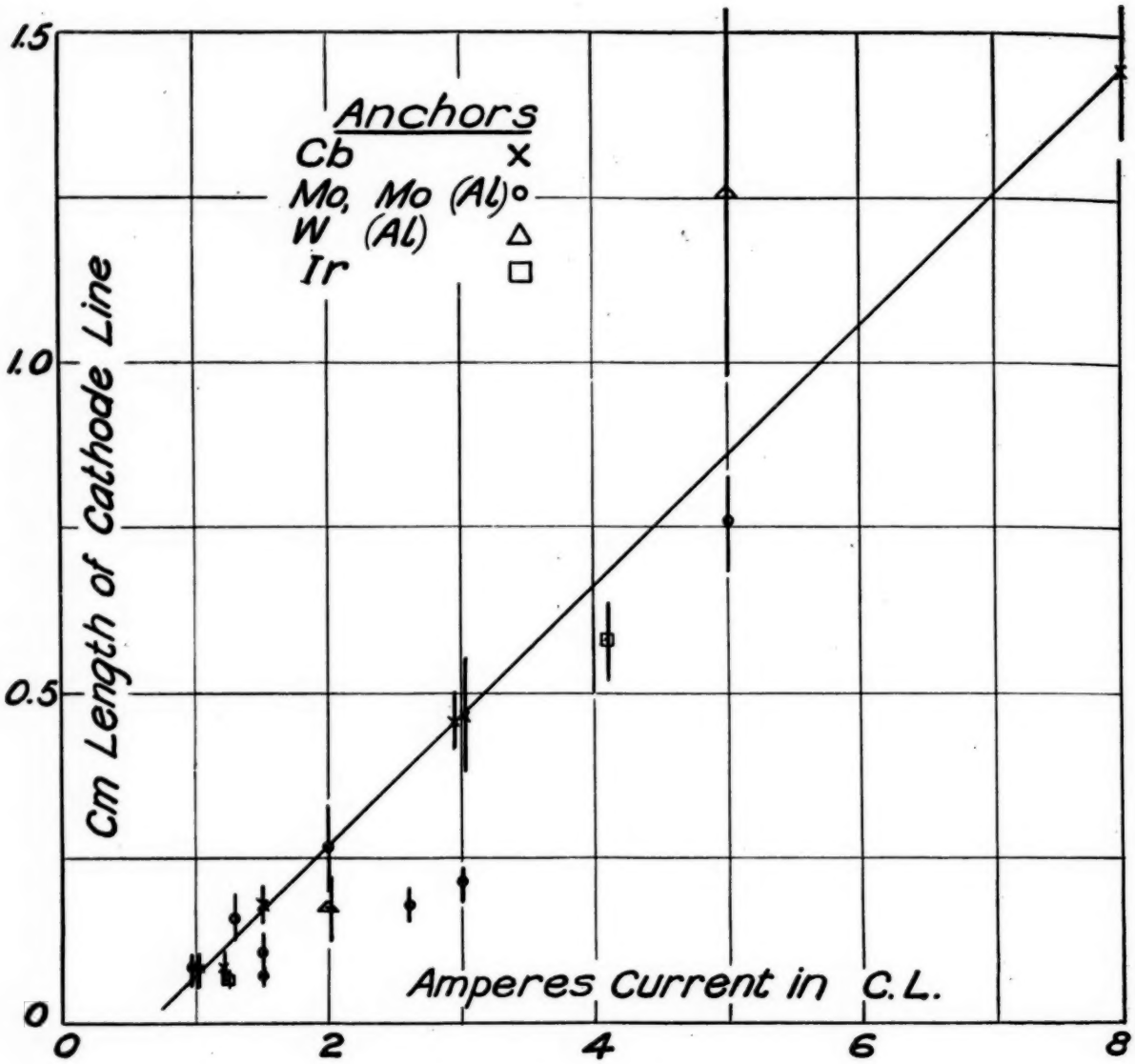

FIG. 8. Cathode line length as a function of current.

each point. The lengths given for Cb 8.0 amp. and W(Al) 2.0 amp. are slightly low, but only slightly, on account of the obstruction in the camera and because in the latter case the C.L. turned a corner on the anchor. In those cases where the current was varying part of the time, those portions of the trace were chosen for measurement at which any effect of the transient in widening the emitting line had died out. The six Cb points lie on a straight line but the 7 Mo points are scattered. The 5-amp. W(Al) trace is seen to be relatively wide despite the above-mentioned under-estimation. Part of this width may well be due to the dispersing action of the waves which have already been invoked to explain the constant velocity off-shoots.

CATHODE LINES LIMITED IN LENGTH

The length of meniscus edge available to a C.L. was conveniently limited to various values by using Mo wires of different diameters projecting vertically through the mercury surface. It was thought possible that with a fine wire the excursions of the emitting areas would be greatly reduced and the smallness of the currents used would avoid undue heating.

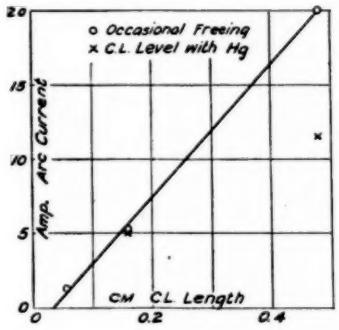

FIG. 9. Current limit of anchoring on cylindrical Mo wires.

Tubes having wires and rods as follows were built: 0.006-inch (0.0152 cm) diam. W in hairpin, 0.007-inch (0.0178 cm) diam. Mo ditto, 0.020-inch (0.051 cm) diam. Mo ditto, 0.060-inch (0.152 cm) diam. Mo rod with a trace of Mg in the Hg.

The C.L. on the 0.060″ rod formed a complete circle about it. As the current was increased, this luminous line depressed the meniscus edge and moved downward. At 11.5 amp. it lay at the same height as the level mercury surface, and surrounding the rod was a uniform trough in the liquid maintained by the pressure originating in the C.L. At 15 amp. the C.L. was well depressed below the surface, the depression deepened just outside the rod and there was a clear tendency for the Hg to fall in over the outer edge, creating a slight agitation over the pool as a whole. At 17.5 amp. the wave motion was strong and at 20 amp. the spot occasionally freed itself. The freeing effect of an increase of temperature was clearly noted. The tube had been cooled by an air blast. When this was cut off with 17.5 amp. flowing, the spot freed itself frequently, but when the blast was turned on again, the spot remained anchored. The behavior of the 0.020″ diam. anchor was similar, surface agitation began at 5.3 amp. and freeing occurred at 6.7 amp. Tests on the 0.006-inch and 0.007-inch wires were less satisfactory, partly because of the difficulty of maintaining with a free spot the low current value which would anchor to such fine wires. By using a large inductance to help maintain the spot, an impermanent anchoring on the 0.007″ filament was observed.

These results have been summarized in Fig. 9 where current is plotted against anchor periphery. The circles show points corresponding to an occasional freeing of the spot, the crosses correspond to a slight agitation of the pool. In view of the rough control of temperature and the presence of Mg in one case and not the others, this plot is only qualitative, yet it establishes an approximate upper value of the current densities which an anchored spot will carry. On plane anchors the limit lies nearer 10 amp./cm than the 40 amp./cm indicated by the figure for small cylinders.

These experiments gave an insight into some of the factors involved in the phenomenon. The force exerted by the cathode line at a differential element of the meniscus edge is a time average of the impulses conveyed as elementary emitting areas pass over the differential element. This force causes a depression of the meniscus which increases with the force. The number of such emitting areas increases with the current so that with a fixed line length the force itself will increase with current. The meniscus edge will continue to be lowered as the current is increased. Observation indicates that the limit to this progress is fixed by the instability of the outer edge of the trough in the mercury. On the other hand, a recent calculation shows that the freeing from the cylindrical anchor occurs at about the current value at which the C.L. tension (force/cm) just overcomes the surface tension of the mercury. It will require further work to decide the matter.

For a fixed force per unit length the amount of depression is greater the lower the surface tension of the liquid. As the mercury is heated, its surface tension decreases and it will reach its unstable configuration at a lower current density. Besides, the decreased surface tension should allow the mercury to break over the outer trough edge with shallower trough. In this way the inability of the uncooled cathode to carry as large currents anchored as the cooled cathode is accounted for.

Operating Characteristics of the FP54 Thermionic Direct-Current Amplifying Tube

P. A. MACDONALD AND W. E. TURNBULL, *Department of Physics, University of Manitoba*

(Received May 16, 1935)

The most suitable characteristics for steady deflection and electrometer use are discussed separately. For the former case it is shown that the mutual conductance may be increased three times the recognized value. When the tube is used as an electrometer a grid current as low as 10^{-17} ampere may be obtained with a voltage sensitivity of 10^{-4} volt/division. The capacity of the grid system being only 3×10^{-12} farad a highly satisfactory electrometer results.

DIRECT-CURRENT amplifiers fall into two main classes, steady deflection instruments and those for the use of which it is necessary to measure the time interval required to alter the charge upon the control grid. The desirable requisites of valves for these two classes of amplification differ considerably and it is the purpose of this communication to point out the characteristics of the FP54 which will allow it to be used at maximum efficiency for each class.

The FP54 is a four-element tube especially developed for direct-current amplification by Metcalf and Thomson.[1] The fourth element is a space charge grid placed between the filament and control grid with the object of decreasing the positive ion current flowing between these elements, i.e., with the object of increasing the grid impedance of the tube. For further details of the tube the reader is referred to the original paper.

STEADY DEFLECTION INSTRUMENT

When used with a steady deflection circuit the valve may be operated at any desired negative bias using an input resistor in series with a negative bias battery or it may be operated at floating grid. The general expression for current amplification is:

$$\frac{di_p}{di}=\frac{G_m}{1/R+1/Z_g},$$

where i is the input current, i_p the plate current, G_m the mutual conductance, R the magnitude of the input resistor and Z_g the reciprocal of the slope of the grid potential *vs.* grid current curve.

From the above equation it will be seen that the sensitivity increases directly with R provided this quantity does not approach Z_g in value. The magnitude of R that may be successfully employed is controlled by two factors, the difficulty in securing high resistors and the desirability of keeping the time constant of the circuit small, since the main value in a direct deflection instrument lies in its rapid response. Resistors exceeding 10^{11} ohms are difficult to obtain and with values exceeding 10^{12} ohms the time constant of the circuit becomes undesirably great. In view of this and the above equation it will be seen that there is nothing to be gained by keeping the input impedance of the tube in excess of 10^{13} ohms. The designers of the tubes have obtained an impedance of 10^{16} ohms at the expense of the mutual conductance which is 25 microamperes/volt. We have examined the characteristics of the valve over a wide range of operating constants in the hope of increasing the mutual conductance by dispensing with some of the unnecessarily high impedance.

Effect of space charge grid potential

The effect of the space charge grid potential upon the mutual conductance was determined by running families of mutual conductance curves for different space charge grid potentials, each family being obtained for one plate potential.

Fig. 1 shows the results of this examination. The inset curves show the manner in which the mutual conductance varies with the space charge grid potential. It will be apparent from these data that the variation is practically independent of plate potential and that a maximum mutual conductance is obtained with approximately 6 volts on the space charge grid.

The family of curves on the right-hand side of the figure shows that the mutual conductance curves approach the axis of zero grid potential as

[1] Metcalf and Thomson, Phys. Rev. **36**, 1489 (1930).

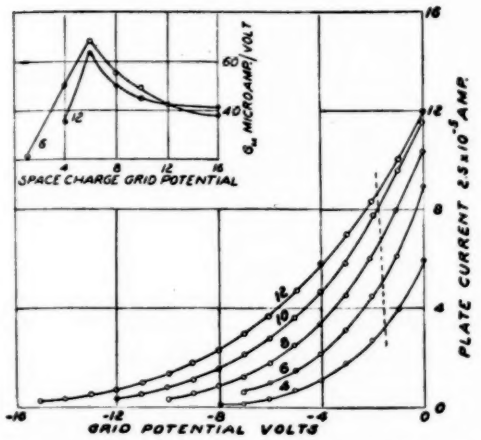

FIG. 1. Data showing the manner in which the space charge grid potential controls the mutual conductance. The numerals on the family of plate current curves denote the space charge grid potential. The inset curves on the left show that a space charge grid potential of six volts gives the maximum mutual conductance at any workable plate potential.

the space charge grid potential is reduced. It will also be seen that any shift in the position of floating grid potential, the locus of which is designated by a broken line, is at the most a second-order effect.

Effect of plate potential

The effect of the plate potential upon the mutual conductance was examined in the same manner as the foregoing and the results are shown in Fig. 2. It will be seen that a plate potential of 8 volts gives the maximum mutual conductance.

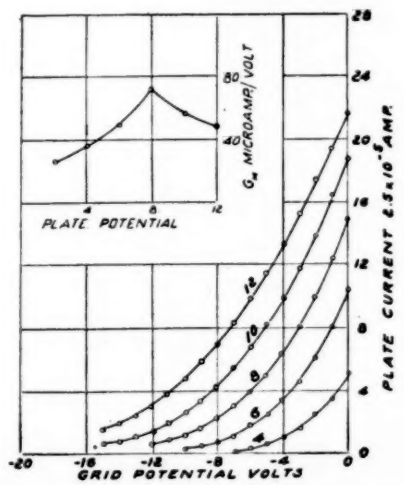

FIG. 2. These data show the manner in which the mutual conductance varies with the plate potential.

Effect of filament potential

Examination of the effect of the filament potential showed that the mutual conductance decreases with this quantity, as would be expected.

Characteristics of input impedance

The effect of the space charge grid and plate potentials upon the grid impedance has been examined by measuring the time required for the control grid current to alter the potential of this grid by a known amount. If the grid be placed at a potential more negative than the floating grid potential and then insulated to other than the grid current, the number N of positive ions flowing to the grid from the filament will decrease as the voltage of the grid becomes more positive according to the equation,

$$dN/dt = -CdE_g/dt.$$

Differentiating with respect to t this may be written

$$di_g/dt = -Cd^2E_g/dt^2. \tag{1}$$

The grid impedance Z_g is defined as

$$Z_g = dE_g/di_g,$$

which may be written

$$di_g/dt = (1/Z_g)\cdot(dE_g/dt). \tag{2}$$

Equating (1) and (2)

$$d^2E_g/dt^2 - (1/Z_gC)\cdot(dE_g/dt) = 0,$$

which has the solution

$$Z_g = \frac{T}{C\log_e[(E_0 - E_f)/(E_g - E_f)]},$$

where E_f is the potential of floating grid, and E_0 the initial grid potential.

On the basis of the above equation the grid impedance was examined over a large range of plate and space charge grid potentials and was found to be always in excess of 10^{13} ohms and in most instances 10^{14}.

As a result it may then be stated that, where the tube is to be used as a steady deflection instrument, the values of the plate and space charge grid potentials giving maximum mutual conductance may be chosen as the most efficient operating values, since the grid impedance under

all working conditions of plate and space charge grid potentials is in excess of that required for maximum current sensitivity.

Combining the results of the examinations of the three parameters of the tube give the most desirable operating characteristics which, along with the values ordinarily used, are reproduced in Table I.

TABLE I.

	Operating characteristics	Rated characteristics
Filament potential	2.5 volts	2.5 volts
Plate potential	8.0 volts	6.0 volts
Space charge grid potential	6.0 volts	4.0 volts
Mutual conductance	70 $\frac{\text{microamperes}}{\text{volt}}$	25 $\frac{\text{microamperes}}{\text{volt}}$
Grid impedance	10^{14} ohms	10^{16} ohms

It will be seen that the slight increase in plate and space charge grid potentials considerably increases the value of the tube as a direct deflection instrument provided the stability of operation has not been upset. The stability of the tube has been examined in all the standard circuits and in every case the recognized limits of thermionic amplification have been approached as readily as with the rated characteristics.

TUBE AS AN ELECTROMETER

The essential difference between an electrometer and a thermionic tube used as an electrometer is the presence of the grid current in the latter case, a factor which considerably alters the significance of the voltage sensitivity of the instrument. The value of the voltage sensitivity in an electrometer lies in decreasing the time of observation so that the lower limit of measurable current is determined only by the time interval which it is feasible to employ in making an observation. The employment of a vacuum tube as an electrometer, however, primarily necessitates reducing the grid current to such a point that it will not mask the presence of the input current, so that considerations of high voltage sensitivity must be subjugated to the realization of this current condition.

While the reduction of the grid current is the fundamental requisite it is somewhat simpler at the outset to consider the question of voltage sensitivity, as the maximum value of this quantity that can be obtained is readily determined from consideration of the fortuitous fluctuations of the tube circuit.

Voltage sensitivity

The maximum voltage sensitivity that may be obtained with any vacuum tube amplifier with a grid capacity of 3×10^{-12} farad, mounted in a vacuum and operated at room temperature is 2×10^{-5} volt, which limit is set by an irregular fluctuation of this magnitude about the zero point. This limit has been carefully determined by Hafstad[2] and his results have been duplicated under many different conditions by the authors both for FP54 and other types of amplifying tubes. This limit is to be attributed to the Schott and Johnson effects, a discussion of which is given by Hafstad. In computing the sensitivity of the vacuum tube electrometer some definition of the limit must be given and for the purposes of the present paper this quantity will be defined as the smallest current that can be measured correct to 10 percent and which causes a scale deflection of one division in sixty seconds. From this definition the maximum voltage sensitivity of a vacuum tube electrometer is 2×10^{-4} volt/division. The sole value of having available a voltage sensitivity in excess of this lies in the fact that it may be reduced to this value by substituting a less sensitive galvanometer in the plate circuit.

Grid current

With these facts in mind attention was directed to the reduction of the grid current by sacrificing some of the mutual conductance of the tube, a condition that can usually be brought about by reducing the filament current. Assuming such to be the case it became desirable to determine the least filament voltage at which the tube would operate with constant characteristics. It was found that with a potential drop of 1.2 volts across the filament absolute constancy of operation could be maintained. This value was accordingly adopted as the most desirable filament voltage for the tube when employed as an electrometer.

A family of characteristic curves for this filament potential is reproduced in Fig. 3, the space

[2] Hafstad, Phys. Rev. **44**, 201 (1933).

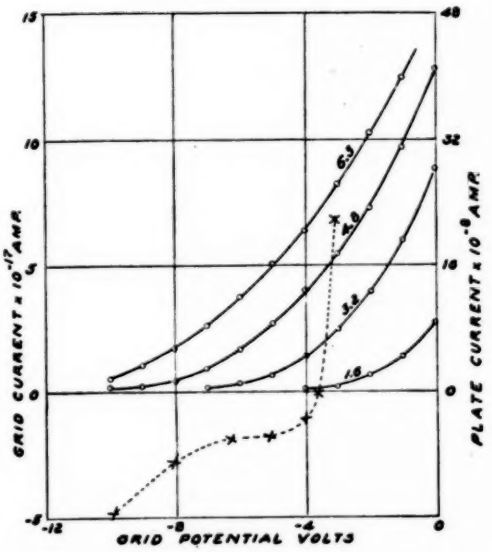

FIG. 3. Family of tube characteristics for use as an electrometer. The circled lines are grid potential *vs.* plate current curves for different plate potentials. The grid current curve is drawn with crosses. The grid current has been reduced to a minimum by reducing the filament current. The resulting reduction of the plate current is no disadvantage as it is still sufficiently large to operate a standard galvanometer and show the irregular fluctuations limiting all thermionic amplifiers.

charge grid potential being 3 volts. This space charge grid potential may be altered a volt either way without making any appreciable difference to the mutual conductance. The intermittent line plotted with crosses in this graph represents a grid current curve obtained with a plate potential of 6 volts. A curve practically identical with this has been obtained with a plate potential of 6 volts and a space charge grid potential of 2 volts, so that this latter value is not at all critical. Plate potentials less than 6 volts reduce the plate current to an undesirable extent and do not appreciably alter the grid current characteristics so that it has been concluded that the data of Fig. 3 for the plate potential of 6 volts give the most desirable characteristics of the tube when used as an electrometer.

The voltage sensitivity of this system will be governed by the sensitivity of the galvanometer in the plate circuit. A galvanometer giving a sensitivity of 10^{-10} amp./mm, at a distance of one meter from the scale is for practical purposes the most sensitive instrument that it is desirable to employ, for while more sensitive instruments are available the sensitivity is obtained at the expense of the period and certain desirable mechanical features.

We have found that it is entirely satisfactory to increase the efficiency of the optical system of the galvanometer to such an extent that a resultant sensitivity ten times greater than the above value is realized. For this purpose an engineer's level is fitted with fine cross hairs and a high power eyepiece; such a telescope enables the scale to be read correct to 0.5 mm at five meters with greater facility than was formerly obtained for a 1 mm scale division at one meter distance.

By using the galvanometer in the above manner and compensating for the plate current through this instrument by using the current from an auxiliary dry cell through a high resistance the data of Table II are obtained giving

TABLE II.

Filament potential	1.2 volts
Plate potential	6.0 volts
Space charge grid potential	3.0 volts
Filament current	70×10^{-3} amp.
Mutual conductance	5×10^{-8} amp./volt.
Voltage sensitivity	10^{-4} volt
Grid impedance at floating grid	10^{16} ohms
Maximum grid impedance	10^{18} ohms
Range of maximum grid impedance	1 volt
Time required for grid to charge up over range of maximum impedance	10^{5} seconds
Operating grid current	10^{-17} amp.
Negative bias	6 volts
Smallest measurable current*	10^{-17} amp.

* The smallest current that can be measured correct to 10 percent in a period of sixty seconds.

the characteristics of the single tube electrometer.

This work has been carried out with the financial assistance of the International Cancer Research Foundation in the Radium Laboratory of the Manitoba Cancer Relief and Research Institute, established in the Department of Physics, University of Manitoba and the authors would like to express their thanks for the courtesies of these institutions.

Some Physico-Mathematical Aspects of Nerve Conduction. II

N. RASHEVSKY, *Department of Physiology, University of Chicago*

(Received June 3, 1935)

In continuation of a previous paper, the equation of propagation of a nerve impulse is studied now under more general assumptions about the physical mechanism of excitation. Instead of H. A. Blair's excitation formula, used previously, a more general formula, proposed by the author elsewhere and having several advantages, is considered. It is found in this case, that the velocity of propagation is not *strictly* constant, but tends asymptotically to a constant value. This asymptotic value is reached practically within 10^{-3} sec. after the propagation of the impulse begins, and the initial velocity is only slightly different from the asymptotic value. The expression for this asymptotic value is in the first approximation identical with the expression deduced previously, and inasmuch as the latter was found to agree with experimental data, the same remains in the present case.

IN a previous paper, published in this journal,[1] we have discussed the physico-mathematical aspects of the process of propagation of a nerve impulse. This process differs essentially from other processes of propagation, studied in physics, by being characterized not by a differential, but by an integral or functional equation. The formula, which we deduced for the velocity of propagation, checks fairly well with available observations. A subsequent analysis of more recent experimental data, made by H. A. Blair[2]) established further agreement with our formula.

As we have seen, the form of the functional equation, which describes the process of propagation, depends on the differential equation, which is assumed to describe the process of excitation by an electric current. In our previous paper,[1] we have chosen as such a differential equation the one proposed by H. A. Blair,[3] as being the simplest equation, which on one hand represents well a number of experimental data, on the other enables us to obtain an exact solution of our integral equation. Blair's equation is however not completely adequate from a biophysical point of view, and we have proposed elsewhere[4] a more general physico-mathematical theory of nerve excitation, which accounts for a number of facts, not accounted for hitherto. In the present paper we shall investigate by the methods used previously[1] the equations of propagation of the nerve impulse, which result from our generalized theory of excitation, and which present some mathematical peculiarities as compared with the formerly studied case.

Our fundamental equations are:[4]

$$\begin{aligned} de/dt &= Ki - k(e-e_0), \\ dj/dt &= Mi - m(j-j_0), \end{aligned} \tag{1}$$

where e and j denote the concentrations of the different types of ions, i the electric current, e_0 and j_0 the initial concentrations of e and j; K, M, k and m are constants. Excitation occurs when the ratio e_0/j_0 exceeds a critical value, which, without any loss of generality, we may put equal to 1. We have:[4]

$$j_0 > e_0; \quad m \ll k; \quad M < K;$$
$$K/k < M/m; \quad Kk > Mm. \tag{2}$$

The same notations are used here as in the previous paper.[1]

As previously we have a time lag t_1, which elapses between the moment $t=0$, at which the excitation at the point $x=0$ occurs, and the beginning of the actual propagation. This time lag t_1 is, however, not expressed any more by Eq. (10) of the previous paper,[1] and we must find the new expression for it.

Consider, as before, a constant current I established at the moment $t=0$, when $e=e_0$ and $j=j_0$. Dividing then the first of Eq. (1) by the second, we have:

$$de/dj = [KI - k(e-e_0)]/[MI - m(j-j_0)] \tag{3}$$

or

$$de/[KI - k(e-e_0)] = dj/[MI - m(j-j_0)]. \tag{4}$$

Hence

[1] N. Rashevsky, Physics **4**, 341 (1933).
[2] H. A. Blair, J. Gen. Physiol. **18**, 123 (1934).
[3] H. A. Blair, J. Gen. Physiol. **15**, 709 (1932).
[4] N. Rashevsky, Protoplasma **20**, 42 (1933).

$$(1/k)\int_{e_0}^{e}\left\{\frac{d[KI-k(e-e_0)]}{[KI-k(e-e_0)]}\right\} = (1/m)\int_{j_0}^{j}\left\{\frac{d[MI-m(j-j_0)]}{[MI-m(j-j_0)]}\right\}, \quad (5)$$

which gives

$$(1/k)\log\{[KI-k(e-e_0)]/KI\} = (1/m)\log\{[MI-m(j-j_0)]/MI\} \quad (6)$$

or

$$\{[KI-k(e-e_0)]/KI\}^m = \{[MI-m(j-j_0)]/MI\}^k. \quad (7)$$

This gives a relation between the value of e at any time, and the corresponding value at the same time of j. Since excitation occurs when $e=j$ therefore the value e^* which e has at this moment is determined as the root of the equation, which is obtained from (7), when we substitute $j=e$. This gives:

$$\{[KI-k(e-e_0)]/KI\}^m = \{[MI-m(e-j_0)]/MI\}^k. \quad (8)$$

Similarly the value j^* which j has at the time when excitation occurs, is given by the root of the equation

$$\{[KI-k(j-e_0)]/KI\}^m = \{[MI-m(j-j_0)]/MI\}^k. \quad (9)$$

Eqs. (8) and (9) express e^* and j^* in terms of the constant quantities I, K, k, M, m, e_0 and j_0. Instead of using for the excitation the criterion $e \gtrless j$, we may therefore say, that *for a case of excitation by a constant current*, excitation occurs when $e \gtrless e^*$; e^* being the root of Eq. (8); or what amounts to the same $j \gtrless j^*$.

The first equation of (1) may be written (for $i=I=$ constant):

$$d(e-e_0)/dt = KI-k(e-e_0) \quad (10)$$

and the requirement $e \gtrless e^*$ is equivalent to

$$e-e_0 \gtrless e^*-e_0 = e_1. \quad (11)$$

But (10) and (11) are formally identical with Blair's equations,[1, 3] in which instead of p we write $e-e_0$, and instead of h we write e_1. Hence, the time necessary for e to reach e^* under the action of a constant current I, is given by:

$$t_1 = (1/k)\log[KI/(KI-ke_1)], \quad (12)$$

which is obtained from Eq. (10) of the previous paper[1] by substituting e_1 for h. Although our Eq. (12) and the Eq. (10) of the previous paper are *formally* identical, there is a great difference between them. Whereas in Eq. (10) of the previous paper h is an independent constant, in our Eq. (12) e_1 is determined by the other constants, in particular by I, according to Eq. (8), together with $e_1=e^*-e_0$.

Similarly we have:

$$t_1 = (1/m)\log[MI/(MI-mj_1)] = (1/k)\log[KI/(KI-ke_1)] \quad (13)$$

with

$$j_1 = j^*-j_0. \quad (14)$$

Eq. (13) gives us a relation between j_1 and e_1, and can be obtained directly from (7).

As in the previous paper,[1] we shall consider the variations of e and j at a point x_0. We have again:[1]

$$i(x_0, t) = Ie^{-\alpha x_0+\alpha u(t)} \quad (15)$$

with[5]

$$\alpha = \{[(\gamma+1)/\gamma](2\rho/\delta\bar{\rho}r)\}^{\frac{1}{2}}, \quad u(t) = \int_{t_1}^{t} v(t)dt. \quad (16)$$

We therefore have:

$$de/dt = KIe^{-\alpha x_0+\alpha u(t)}-k(e-e_0), \quad dj/dt = MIe^{-\alpha x_0+\alpha u(t)}-m(j-j_0), \quad (17)$$

which give upon integration

$$e = e_0+C_1e^{-kt}+KIe^{-kt-\alpha x_0}\int_{t_1}^{t} e^{\alpha u(t)+kt}dt, \quad (18)$$

$$j = j_0+C_2e^{-mt}+MIe^{-mt-\alpha x_0}\int_{t_1}^{t} e^{\alpha u(t)+mt}dt. \quad (19)$$

C_1 and C_2 are constants, determined by the values $e(x_0, t_1)$ and $j(x_0, t_1)$ of e resp. j at the

[5] In the previous paper, reference 1, in the expression for α the factor $(\gamma-1)/\gamma$ has been given erroneously instead of $(\gamma+1)/\gamma$. The error is due to the circumstance that in Eq. (2) reference 1 we must have $di/dx = -di'/dx$, i and i' having opposite directions. The final results are not invalidated by this mistake, except that for $\gamma=1$ we would get $\alpha=0$, which is absurd. I am indebted to Professor A. V. Hill for calling my attention to this error.

point x_0 at the time $t=t_1$. Since between $t=0$ and $t=t_1$ the current at x_0 has the constant value $Ie^{-\alpha x_0}$, and at $t=0$ $e(x_0)$ and $j(x_0)$ equal respectively to e_0 and j_0, therefore we obtain the variation of e resp. j at x_0, between $t=0$ and $t=t_1$ by integrating (17), and find[1]

$$\left.\begin{aligned} e(x_0, t) &= e_0+(KIe^{-\alpha x_0}/k)(1-e^{-kt}), \\ j(x_0, t) &= j_0+(MIe^{-\alpha x_0}/m)(1-e^{-mt}). \end{aligned}\right\} \quad (20)$$

To find $e(x_0, t_1)$ and $j(x_0, t_1)$ we must substitute in (20) for t_1 the expression (12) resp. (13). This gives after elementary calculations:[1]

$$e(x_0, t_1)=e_0+e_1e^{-\alpha x_0}; \quad j(x_0, t_1)=j_0+j_1e^{-\alpha x_0}. \quad (21)$$

Hence C_1 and C_2 are determined by the conditions:

$$\begin{aligned} e_0+C_1e^{-kt_1} &= e_0+e_1e^{-\alpha x_0}; \\ j_0+C_2e^{-mt_1} &= j_0+j_1e^{-\alpha x_0}, \end{aligned} \quad (22)$$

the values of the integrals in Eq. (18) and (19) being zero for $t=t_1$. From (22) we find:

$$\begin{aligned} C_1 &= [e_1KI/(KI-ke_1)]e^{-\alpha x_0}; \\ C_2 &= [j_1MI/(MI-mj_1)]e^{-\alpha x_0}. \end{aligned} \quad (23)$$

Introduced into (18) and (19) this gives:

$$\begin{aligned} e(x_0, t) &= e_0+[e_1KI/(KI-ke_1)]e^{-\alpha x_0-kt}+KIe^{-\alpha x_0-kt}\int_{t_1}^{t} e^{\alpha u(t)+kt}dt, \\ j(x_0, t) &= j_0+[j_1MI/(MI-mj_1)]e^{-\alpha x_0-mt}+MIe^{-\alpha x_0-mt}\int_{t_1}^{t} e^{\alpha u(t)+mt}dt. \end{aligned} \quad (24)$$

The excitation reaches x_0 when $e(x_0, t)=j(x_0, t)$. Hence the time, when this happens is given by the equation:

$$\begin{aligned} e_0+[e_1KI/(KI-ke_1)]e^{-\alpha x_0-kt}+KIe^{-\alpha x_0-kt}\int_{t_1}^{t} e^{\alpha u(t)+kt}dt \\ = j_0+[j_1MI/(MI-mj_1)]e^{-\alpha x_0-mt}+MIe^{-\alpha x_0-mt}\int_{t_1}^{t} e^{\alpha u(t)+mt}dt. \end{aligned} \quad (25)$$

By exactly the same line of argument as before,[1] we now find the functional equation for $u(t)$ by substituting in (25) $u(t)$ for x_0. Performing this substitution and making some rearrangements, we find:

$$\begin{aligned} e_0+[e_1KI/(KI-ke_1)]e^{-\alpha u(t)-kt}+KIe^{-\alpha u(t)-kt}\int_{t_1}^{t} e^{\alpha u(t)+kt}dt \\ -j_0-[j_1MI/(MI-mj_1)]e^{-\alpha u(t)-mt}-MIe^{-\alpha u(t)-mt}\int_{t_1}^{t} e^{\alpha u(t)+mt}dt=0. \end{aligned} \quad (26)$$

Multiplying by $e^{\alpha u(t)+kt}$ we find:

$$\begin{aligned} e_0e^{\alpha u(t)+kt}+e_1KI/(KI-ke_1)+KI\int_{t_1}^{t} e^{\alpha u(t)+kt}dt-j_0e^{\alpha u(t)+kt} \\ -[j_1MI/(MI-mj_1)]e^{(k-m)t}-MIe^{(k-m)t}\int_{t_1}^{t} e^{\alpha u(t)+mt}dt=0. \end{aligned} \quad (27)$$

Differentiating (27) with respect to t and remembering, that[1] $du(t)/dt=v(t)$, we find:

$$e_0[\alpha v(t)+k]e^{\alpha u(t)+kt}+KIe^{\alpha u(t)+kt}-j_0[\alpha v(t)+k]e^{\alpha u(t)+kt}-[(k-m)j_1MI/(MI-mj_1)]e^{(k-m)t}$$
$$-MIe^{\alpha u(t)+kt}-(k-m)MIe^{(k-m)t}\int_{t_1}^{t}e^{\alpha u(t)+mt}dt=0. \quad (28)$$

Multiplying with $e^{-(k-m)t}$ and differentiating again with respect to t, we find after simple rearrangements, and writing for brevity v instead of $v(t)$:

$$\{(e_0-j_0)\alpha(dv/dt)+(e_0-j_0)(\alpha v+k)(\alpha v+m)$$
$$+(K-M)I(\alpha v+m)$$
$$-(k-m)MI\}e^{\alpha u(t)+mt}=0. \quad (29)$$

Eq. (29) means, that the expression in the braces must be zero, and this gives us a differential equation for v, which after elementary rearrangements takes the form:

$$\alpha dv/dt=-\alpha^2v^2-[(m+k)-(K-M)I/(j_0-e_0)]\alpha v-[mk+I(Mk-Km)/(j_0-e_0)]. \quad (30)$$

Introducing a new variable

$$x=\alpha v \quad (31)$$

and putting

$$(m+k)-(K-M)I/(j_0-e_0)=-a,$$
$$mk+I(Mk-Km)/(j_0-e_0)=b, \quad (32)$$

we have:

$$dx/dt=-x^2+ax-b. \quad (33)$$

Eq. (33) shows, that dx/dt, when plotted as a function of x, is represented by a parabola, with its apex turned upwards. If the equation

$$-x^2+ax-b=0 \quad (34)$$

has no real roots, then $dx/dt=\alpha dv/dt<0$ for any value of $x=\alpha v$. This means, that no propagation of the nerve impulse can occur at all, for otherwise v would eventually become negative. If, however, Eq. (34) has two real roots, x_1 and $x_2>x_1$, which is the case, as we shall presently see, then $dx/dt<0$ for $x<x_1$ and $x>x_2$; but $dx/dt>0$ for $x_1<x<x_2$. For $x=x_1$ or $x=x_2$, $dx/dt=0$. This means, that if the initial value v_0 of the velocity (that is the velocity at the moment $t=t_1$) is such that $x_0=\alpha v_0<x_1$, then x, resp. v will be continuously decreasing, which again is physically impossible. If $x_1<x_0=\alpha v_0<x_2$, then dx/dt is positive and x increases, reaching asymptotically the value x_2. If $x_0=\alpha v_0>x_2$, then dx/dt is negative; x decreases reaching again asymptotically the value x_2. x_2 is therefore the *only stable* asymptotic value, physically possible. We shall presently see, that actually $x_0>x_1$, so that the velocity of propagation tends asymptotically to the stable constant value x_2. The correspondent asymptotic value of $v=x/\alpha$ we shall denote by v_a. Thus $\alpha v_a=x_2$.

If the two roots x_1 and x_2 of (34) coincide, so that $x_1=x_2=x^*$, then, as is easily seen, $v^*=x^*/\alpha$ is not a stable asymptotic value, for an infinitesimal decrease of x, resp. v would make it decrease still further. This case, as we shall see, does not actually occur.

The variation of x, resp. v with t is found by integrating (33). We have:

$$\int dx/(-x^2+ax-b)=t+C_1, \quad (35)$$

C_1 being a constant of integration. The integral in (35) is equal[6] to

$$(1/\sqrt{\Delta})\log[(-2x+a-\sqrt{\Delta})/(-2x+a+\sqrt{\Delta})] \quad (36)$$

with

$$\Delta=a^2-4b>0.$$

Since, because of (2), $a>0$, therefore, if $\Delta>0$

$$x_1=(1/2)(a-\sqrt{\Delta}); \qquad x_2=(1/2)(a+\sqrt{\Delta}), \quad (37)$$

so that (35) may be written:

$$(1/\sqrt{\Delta})\log[(x_1-x)/(x_2-x)]=t+C_1 \quad (38)$$

or, solving for x:

$$x=\alpha v=(Ax_2e^{\sqrt{\Delta}t}-x_1)/(Ae^{\sqrt{\Delta}t}-1);$$
$$A=e^{\sqrt{\Delta}C_1}. \quad (39)$$

The constant A is determined from the condition, that for $t=t_1$, $x=x_0=\alpha v_0$. This gives:

$$A=(x_1-x_0)e^{-\sqrt{\Delta}t_1}/(x_2-x_0)=A_1e^{-ct_1} \quad (40)$$

with

[6] O. B. Peirce, *A Short Table of Integrals*, third edition (Ginn and Co., 1929), p. 10.

$$A_1=(x_1-x_0)/(x_2-x_0); \qquad c=\sqrt{\Delta}. \quad (41)$$

If $x_1<x_0<x_2$, then $A_1<0$, with increasing t, x tends, according to (39), asymptotically to x_2. If $x_0>x_2$, then $A>0$, and for $t=t_1$, $Ae^{ct}=A_1>1$. The denominator in (39) remains always finite for $t>t_1$, and again x tends asymptotically to x_2. If $x_0<x_1$, for $t>t_1$, then $A>0$, but for $t=t_1$, $Ae^{ct}=A_1<1$. As t increases Ae^{ct} approaches 1. For $t=-(1/c)\log A$ the denominator of (39) becomes zero and x positive or negative infinite, depending on the values of x_1 and x_2. All this bears out our previous analysis of Eq. (33). For $x_0=x_2$, A_1 becomes infinite. Inversely, if $A_1>1$, then $x_0>x_2$, if $A_1<0$, then $x_1<x_0<x_2$, if $0<A_1<1$, then $x_0<x_1$. As $|A_1|$ increases x_0 tends to x_2.

The value of the constant A is actually found by substituting Eq. (39) into the functional Eq. (26). The requirement that (26) then becomes an identity for all values of $t\geqq t_1$ determines the value of A, and hence of $x_0=\alpha v_0$. Before proceeding with the calculations proper, we must establish a few auxiliary formulae, which will be needed later.

First of all, we find by simple rearrangement, that Eq. (30) can also be written thus:

$$e_0-j_0+KI/(k+x)-MI/(m+x)=0 \quad (42)$$

or, on account of (11):

$$(j_1-e_1)+KI/(k+x)-MI/(m+x)=0. \quad (43)$$

Eq. (43) gives:

$$j_1-MI/(m+x)=e_1-KI/(k+x). \quad (44)$$

Consider the identity:

$$[e_1-KI/(k+x_1)][e_1-KI/(k+x_2)] =[e_1-KI/(k+x_1)][e_1-KI/(k+x_2)], \quad (45)$$

in which x_1 and x_2 are, as before, the roots of Eq. (30), or which is the same, of (42), (43) or (44). On account of (44), the identity (45) can also be written thus:

$$[e_1-KI/(k+x_1)][j_1-MI/(m+x_2)] =[j_1-MI/(m+x_1)][e_1-KI/(k+x_2)] \quad (46)$$

or

$$\frac{e_1-KI/(k+x_1)}{e_1-KI/(k+x_2)}=\frac{j_1-MI/(m+x_1)}{j_1-MI/(m+x_2)}, \quad (47)$$

which can also be written

$$(k+x_2)[e_1(k+x_1)-KI]/(k+x_1)[e_1(k+x_2) -KI]=(m+x_2)[j_1(m+x_1)-MI]/ (m+x_1)[j_1(m+x_2)-MI]. \quad (48)$$

Furthermore, we have from (13):

$$\begin{aligned} KI/(KI-ke_1)&=e^{kt_1}; \quad e_1=KI(1-e^{-kt_1})/k;\\ MI/(MI-mj_1)&=e^{mt_1}; \quad j_1=MI(1-e^{-mt_1})/m. \end{aligned} \quad (49)$$

We now proceed to calculate A. By elementary integration, making use of the relation

$$x_2-x_1=\sqrt{\Delta}=c, \quad (50)$$

which follows from (37), we find

$$\alpha u(t)=\alpha\int_{t_1}^{t}v(t)dt=\int_{t_1}^{t}x_2dt=\log\left[(Ae^{ct}-1)/(Ae^{ct_1}-1)\right]+x_1(t-t_1). \quad (51)$$

From (51) we find, after some elaborate, but also elementary calculations,

$$\int_{t_1}^{t}e^{\alpha u(t)+kt}dt=Ae^{-x_1t_1}(e^{(k+x_2)t}-e^{(k+x_2)t_1})/(Ae^{ct_1}-1)(k+x_2) -e^{-x_1t_1}(e^{(k+x_1)t}-e^{(k+x_1)t_1})/(Ae^{ct_1}-1)(k+x_1) \quad (52)$$

and

$$\int_{t_1}^{t}e^{\alpha u(t)+mt}dt=Ae^{-x_1t_1}(e^{(m+x_2)t}-e^{(m+x_2)t_1})/(Ae^{ct_1}-1)(m+x_2) -e^{-x_1t_1}(e^{(m+x_1)t}-e^{(m+x_1)t_1})/(Ae^{ct_1}-1)(m+x_1). \quad (53)$$

Substituting (52), (51) and (53) into (26) and making use of (49) and (50), we find after rather laborious rearrangements:

$$Ae^{ct}[e_0-j_0+KI/(k+x_1)-MI/(m+x_2)]-[e_0-j_0+KI/(k+x_1)-MI/(m+x_1)]$$
$$+\{Ae^{(k+x_2)t_1}-Ae^{x_2t_1}-A[k/(k+x_2)]e^{(k+x_2)t_1}-e^{(k+x_1)t_1}+e^{x_1t_1}$$
$$+[k/(k+x_1)]e^{(k+x_1)t_1}\}(KI/k)e^{-(k+x_1)t}-\{Ae^{(m+x_2)t_1}-Ae^{x_2t_1}-A[m/(m+x_2)]e^{(m+x_2)t_1}$$
$$-e^{(m+x_1)t_1}+e^{x_1t_1}+[m/(m+x_1)]e^{(m+x_1)t_1}\}(MI/m)e^{-(m+x_1)t}=0. \quad (54)$$

The first two terms of the left-hand side of (54) are zero because of (42). In order to make the third term zero for all values of t the expression in the corresponding braces must be zero, which gives:

$$A(e^{(k+x_2)t_1}-e^{x_2t_1}-[k/(k+x_2)]e^{(k+x_2)t_1})-e^{(k+x_1)t_1}+e^{x_1t_1}+[k/(k+x_1)]e^{(k+x_1)t_1}=0 \quad (55)$$

or

$$A\left(\frac{x_2}{k+x_2}e^{(k+x_2)t_1}-e^{x_2t_1}\right)=\frac{x_1}{k+x_1}e^{(k+x_1)t_1}-e^{x_1t_1}. \quad (56)$$

Dividing both sides of (56) by e^{x_1t} and making use of (50), we find:

$$Ae^{ct_1}\left(\frac{x_2}{k+x_2}e^{kt_1}-1\right)=\frac{x_1}{k+x_1}e^{kt_1}-1. \quad (57)$$

Substituting for e^{kt_1} its value from (49) we find after simple rearrangements:

$$A=e^{-ct_1}(k+x_2)[e_1(k+x_1)-KI]/(k+x_1)[e_1(k+x_2)-KI]. \quad (58)$$

In quite a similar way we find in order to make the fourth term of (54) equal to zero for all values of t, that the expression in the corresponding braces must be zero, which gives:

$$A=e^{-ct_1}(m+x_2)[j_1(m+x_1)-MI]/(m+x_1)[j_1(m+x_2)-MI]. \quad (59)$$

But on account of (48), expressions (58) and (59) are identical. Hence, when A has the value given by (58) or (59) then the substitution of (39) into the fundamental functional equation (26) makes the latter an identity. This also constitutes a check of the correctness of our solution (39).

Eqs. (39), (37) and (58) or (59) *represent the exact and complete solution of our problem.*

We must now give approximate formulae, which will enable us to calculate the actual numerical value of the velocity of propagation v. We have seen,[4] that k in our Eqs. (1) has with a great approximation the same value as the k calculated from Blair's equation.[1, 3] It is of the order of magnitude of 10^3 sec.$^{-1}$ The value of m determines the time, which it takes for j to reach its asymptotic value under the action of a suddenly established constant current.[4] This time is closely related[4] to the time of the "reversal of electrotonus." This time being of the order of magnitude of several minutes, it follows[4] that $m\sim10^{-2}$ sec.$^{-1}$ or even smaller. Hence $m+k\sim k$.

The expression (32) for b may be written thus:

$$b=mk[1+(M/m-K/k)I/(j_0-e_0)]. \quad (60)$$

$(M/m-K/k)I/(j_0-e_0)$ is a measure[4] of the electrotonic change of the excitability. There are no exact data available for this quantity, but in general it is of the order of magnitude of one. Hence $b\sim10$.

The coefficient a in (32) and (33) can furthermore be expressed in terms of the rheobase R (liminal exciting current). Referring to Fig. 1 of a previous paper,[4] we see, that when the current I is equal to the rheobase R, the curves

$$e=e_0+(KI/k)(1-e^{-kt})$$

and

$$j=j_0+(MI/m)(1-e^{-mt}) \quad (61)$$

are tangent to each other at a moment which we shall denote by t^*. Hence

$$KRe^{-kt^*}=MRe^{-mt^*} \quad (62)$$

and

$$e_0+(KR/k)(1-e^{-kt^*})=j_0+(MR/m)(1-e^{-mt^*}). \quad (63)$$

From (62) we find:

$$t^* = [1/(k-m)] \log (K/M) \qquad (64)$$

and substituting this into (63):

$$e_0 + (KR/k)[1-(M/K)^{k/(k-m)}] = j_0 + (MR/m)[1-(M/K)^{m/(k-m)}], \qquad (65)$$

which is a linear equation determining R. $m/(k-m)$ being of the order of 10^{-5}, the expression in square brackets on the right-hand side of (65) is very near to zero, and can be neglected, MR/m being of the same order of magnitude as j_0. On the other hand with the same approximation $k/(k-m)=1$. Introducing this into (65) we find

$$R = (j_0 - e_0)k/(K-M). \qquad (66)$$

Introducing this into (32) and writing k for $k+m$, we find:

$$a = [(I-R)/R]k > 0. \qquad (67)$$

Data by H. A. Blair[2] show that I is between 2 and 4 times R. Hence $a \sim 10^3$.

With this value of a, and the above found value for b we see, referring to Eq. (37), that with the same approximation

$$\sqrt{\Delta} = a; \qquad x_1 = 0; \qquad x_2 = a. \qquad (68)$$

(68), (67) and (31) now give for the asymptotic value of v:

$$x_2/\alpha = v_a = (I-R)k/\alpha R, \qquad (69)$$

which is identical with the expression derived in our previous paper.[1] The rate, at which this asymptotic value (69) is approached, is determined, according to (39) by $\sqrt{\Delta} = a$. From (67) we see that the asymptotic value is very nearly reached within the first 10^{-3} of a second.

Now we must calculate the constant A, resp. A_1 to find the initial velocity v_0. From (58) and (40) we have:

$$A_1 = (k+x_2)[e_1(k+x_1) - KI]/(k+x_1)[e_1(k+x_2) - KI], \qquad (70)$$

which can also be written:

$$A_1 = [KI/(k+x_1) - e_1]/[KI/(k+x_2) - e_1]. \qquad (71)$$

Referring again to Fig. 1 of a previous paper,[4] we see that if the inequalities (2) hold, then e_1 is slightly larger than $j_0 - e_0$, and is smaller than KR/k. As $j_0 - e_0$ differs very slightly from KR/k, e_1 is very close to that quantity. If $e_1 = KR/k$, then, on account of (69) we would have $KI/(k+x_2) = e_1$, $KI/(k+x_1) > e_1$. A_1 would become infinite, which would mean $v_0 = v_a$, or in other words, a strictly constant velocity of propagation. However $KI/(k+x_2)$ being only approximately equal to e_1, A_1 is finite, but very large. Since $x_1 = 0$, and $x_2 > k$, therefore at any rate $KI/(k+x_1) > 0$. Hence, when $KI/(k+x_2)$ is slightly larger than e_1, $A_1 < 0$; $|A_1| \gg 1$; v_0 is positive, but slightly smaller than v_a. If $KI/(k+x_2)$ is slightly smaller than e_1, $A_1 \gg 1$, and $v_0 > v_a$. Which of the two cases does actually occur, and whether in particular $KI/(k+x_2)$ may happen to be exactly equal to e_1, can be answered only upon a more detailed investigation of the exact values of all the constants of Eq. (1). This problem, being more a biological than a physical one, falls out of the scope of the present paper.

At any rate with a great approximation, the velocity of propagation is uniform, and is found to be expressed by a formula which agrees with experimental data. Only further considerable refinement of the experimental technique will enable to observe those slight deviations from uniformity, which are required by this general theory.

We may add, that an approximate expression for e_1 can be obtained by expanding both sides of (13) and omitting terms of power higher than 2. After somewhat lengthy but quite elementary calculations, this shows that approximately $e_1 = KI/(k+x_2)$, and this confirms in a somewhat more rigorous way our conclusions.